Multiscale Foreign Exchange Dynamics in India: A Wavelet Approach for four major currencies*

Vimarsh Padha[2] Aditi Chaubal [3]

Abstract

Exchange rate fluctuations significantly impact forex market participants, making it crucial to understand the asymmetrical responses and spillover effects across different time horizons. This study examines the multiscale properties of Indian exchange rate returns for the Indian Rupee (INR) against the US Dollar (USD), Euro (EUR), British Pound (GBP), and Japanese Yen (JPY) from January 6, 1999, to September 5, 2023. Using wavelet multiresolution analysis combined with non-linear methods, we identify significant volatility spillovers and persistent long-term effects. Wavelet and spectral variance analyses reveal notable fluctuations during financial crises, such as the taper tantrum, while wavelet coherence and phase difference reveal INR-USD's leading influence on other currency pairs. Hurst exponent analysis highlights long memory at broader scales and mean-reversion over shorter intervals (2–32 days), while chaos is found to be statistically insignificant. . The presence of volatility spillovers and long memory suggests inefficiencies in price discovery, particularly for more volatile currency pairs like INRJPY and INREUR, while stable pairs like INRUSD and INRGBP exhibit relatively efficient market behavior.Traditional models like ARMA and GARCH provide superior forecasts for stable pairs (INRUSD, INRGBP), while wavelet-augmented models, especially Hybrid LSTM-Wavenet, outperform for volatile currencies like INRJPY and INREUR by capturing complex, multiscale patterns. These results offer critical insights for risk management and policy formulation, highlighting the importance of multiscale analysis and machine learning techniques in enhancing the exchange rate forecasting and understanding market dynamics in globally integrated financial systems.

JEL Classification: C14, C22, C45, C58, F31, G17

Keywords: Wavelets, Forecasting Models, Long Memory, Nonlinear Dynamics, Multiscale Analysis, Price Discovery

---

* An earlier version of the manuscript was presented at the 8th International Workshop on Financial Markets and Nonlinear Dynamics in Paris (May 30-31, 2024). We are sincerely grateful to Prof. Fredj Jawadi, Prof. Gilles Dufrenot for their insightful comments along with those given by participants at the conference, which have greatly improved the manuscript.
[2] Department of Economics, Indian Institute of Technology Bombay, Powai, Mumbai, 400076, India
[3] Department of Economics, Indian Institute of Technology Bombay, Powai, Mumbai, 400076, India

1. Introduction

Exchange rates exhibit time-varying and clustered volatility, characterized by prolonged periods of stability or turbulence, occasionally disrupted by sudden, sharp fluctuations (Engle, 1982). These fluctuations have significant impacts on various stakeholders in forex markets, often leading to asymmetric outcomes. Due to the differing time horizons of market participants, exchange rate volatility can cause severe spillover effects on both individual investors and financial institutions. This impact is evident in historical financial crises across both advanced and emerging markets, such as the Latin American debt crisis of the 1980s, the Mexican peso crisis of the 1990s, the Asian financial crisis of the late 1990s, as well as more recent events like the Covid-19 pandemic and the Russia-Ukraine conflict (Bekaert, 1995; Edwards et al., 2002; De Grauwe and Grimaldi, 2006; Yildirim et al., 2016; Venkatesh et al., 2020; Yueh, 2023).

The concept of time horizon, grounded in Milton Friedman's Permanent Income Hypothesis, emphasizes the importance of different time scales in economic processes (Friedman, 1957). This concept extends to time-frequency applications (Ramsey and Lampart, 1998; Bekiros et al., 2013). Muller's Heterogeneous Market Hypothesis highlights that market participants interpret the same information differently based on their operating time scales, influencing market dynamics (Müller et al., 1997; Gençay et al., 2001a; Hommes, 2006).

Scale plays a crucial role in forex markets, where stakeholders operate over varying time horizons with diverse objectives (Ramsey, 2002; Corsi, 2009; Selcuk and Gençay, 2006). For instance, a central bank's policy announcement may immediately impact forex prices due to traders' rapid responses while affecting long-term investor sentiment. Thus, factors driving changes in short-run (such as reactions to exchange rate volatility) differ from those driving long-term changes like inflation control, underscoring the importance of scale in economic decision-making (Gençay et al., 2001; Mehra and Sawhney, 2010; Yu, 2013; Ashley et al., 2015; Pir, 2022).

Efficient price discovery is essential for well-functioning financial markets. Increased financial integration[4], the growing size of economies, and technological advances have bridged information asymmetry, leading to volatility spillovers[5] and contagion[6] effects (Karolyi, 2003; Rigobon, 2003; Forbes,

[4] The forex market's scale has grown rapidly, with average daily turnover increasing from USD 5.8 trillion in 2019 to USD 6.6 trillion in 2022. Emerging market economies (EMEs) play a notable role, accounting for 25% of the total turnover (McGuire 2022).

[5] Refers to "*the transmission of economic shocks from one country to another through trade, financial, and confidence channels, affecting other countries' economic activities, prices, and policies*." (Eichengreen et al., 2011).

[6] Refers to "*the spreading of a crisis from one country to another through a financial link*." (Claessens et al. (2013). *Pure* contagion refers to the excessive transmission of shocks that go beyond any individual disturbances or fundamental connections (Eichengreen et al., 1996; Forbes & Rigobon, 2002). On the other hand, *fundamentals*-based contagion is spread through financial market integration and trade linkages or interdependence (Calvo & Reinhart, 1996).

2004; Bekaert et al., 2005). The interconnectedness of global financial markets suggests that any new information, regardless of where it originates, is rapidly incorporated into asset prices globally (Fama (1970). Volatile markets often show price co-movements and contagion risks, making price discovery challenging and increasing the difficulty for stakeholders in accurately assessing risk expectations and forecasting(Gong et al., 2023). This affects both the real economy and financial markets, thus challenging market efficiency. Examining volatility[7] spillovers, and modelling properties such as long memory[8] and chaos[9], is thus critical for understanding market fluctuations as it influences investment decisions at various horizons (Kodres and Pritsker, 2002; Diebold and Yilmaz, 2009).

Traditional linear time series methods have been used for analyzing forex market volatility by imposing assumptions of time-invariant properties, which can lead to information loss. Conditional heteroskedasticity models like ARCH (Autoregressive Conditional Heteroskedasticity Model), GARCH (Generalised Autoregressive Conditional Heteroskedasticity Model), and stochastic volatility models are the commonly used models to model volatility in financial markets (Andersen and Bollerslev, 2018). However, wavelet analysis provides a more robust method by simultaneously examining time series in both temporal and frequency dimensions, without the need for restrictive assumptions like time invariant moments of a process (Crowley, 2007; Pir, 2022).Wavelets, described as "small waves that grow and decay within a limited time" (Percival and Walden, 2000, pp.2), enable the simultaneous extraction of time and frequency information. This is crucial for capturing the non-stationary behaviour of macroeconomic processes influenced by trends, cycles, and shocks from structural breaks or unforeseen events (Ramsey, 2002; Nachane, 2018).

Over the past three decades, wavelet analysis has gained prominence in economics and finance due to application of the methods by Ramsey and Zhang (1997), Gençay et al. (2001), Ramsey (2002), Schleicher (2002), Connor and Rossiter (2005), Gallegati and Gallegati (2007), Crowley et al. (2021, 2024) etc. Advances in spectral analysis, multiresolution analysis, and orthogonal wavelet bases have shown the effectiveness of wavelets in handling non-stationary data through time-localized decomposition, capturing transient features, and enabling a deeper understanding of underlying patterns that traditional methods might miss. (Grossman and Morlet, 1984; Mallat, 1989; Meyer, 1992; Daubechies, 1992; Percival and Walden, 2000; Gençay et al., 2001; Conlon and Cotter, 2012).

[7] Variance of an asset's returns, given past returns and past conditional variances (Bollerslev, 1986).
[8] Slow hyperbolic decay in autocorrelation rather than rapid exponential decay (Baillie, 1996).
[9] Refers to random behaviour produced by a purely deterministic, nonlinear system, with unpredictable periodicity and sensitivity to initial conditions (Gleick, 2008; Kantz and Schreiber, 1997).

Wavelets can be used to decompose financial time series across various scales, making them useful for examining relationships that vary with scale. Recent literature highlights the use of wavelets for predicting GDP growth, equity prices, oil prices, forex volatility, money growth, and inflation (Zhang, 2003; Yousefi et al., 2005; Crowley, 2007; Pir, 2022; Kılıç, et al. 2023). There remains significant scope for using wavelet-based approaches to examine multiscale properties in the Indian forex market for more effective prediction.

This study thus aims to bridge this gap by employing wavelet multiresolution analysis (MRA) with nonlinear time series measures and a hybrid LSTM (Long Short Term Memory) - Wavenet model. Our focus is to study the multiscale properties and better predict the returns across scales compared to traditional approaches[10]. This approach helps analyse complex economic dynamics which would provide valuable insights for monitoring systemic risk, developing policies, and regulating globally integrated financial markets.

The objective is to determine if forecasting exchange rates by accounting for different time horizons using a wavelet-based approach outperforms traditional time series models. We aim to achieve this by implementing the following steps:

1. Examine the multiscale properties in forex markets by analysing the Indian Rupee (INR) returns relative to four major exchange rates: the US Dollar (USD), the British Pound (GBP), the Euro (EUR), and the Japanese Yen (JPY). This is done using MODWT (Maximal Overlap Discrete Wavelet Transform) which decomposes each series into sub-scales.
2. Test for spillovers during periods of distress and normalcy (identified using PELT method), using DCC GARCH.
    a. assess whether contagion and interdependence is pronounced in the exchange rate returns.
    b. compare the findings of DCC GARCH with spectral and wavelet variance analysis during periods of financial crises.
3. Examine the extent of contagion across the major Indian exchange rates using wavelet coherence and correlation identified in step 2, especially during periods of normalcy and distress.
4. Test for long memory and chaotic behaviours in exchange rate returns at both the aggregate and across different scales.
5. Compare wavelet-based forecast performance with those obtained from traditional time series approaches at aggregate level and across scales.

[10] In order to maintain the brevity of the paper, our study does not focus on the economic models of exchange rate determination (see Dua and Ranjan (2011), for detailed review). Application to these models provides scope for further research.

This study contributes to the literature in several key ways. First, we use time-series approaches as precursors to applying the DCC GARCH model to examine volatility spillovers and interdependence, followed by spectral and wavelet variance analyses of exchange rate returns, revealing scale-wide volatility dynamics and frequency-specific causality. Additionally, we examine multiple forms of applicable wavelets for implementation. We test for long memory and chaos at different scales, which has implications for market efficiency. Finally, we compare forecasts obtained using traditional time series methods with those obtained using new hybrid LSTM-Wavenet model. This is done to examine whether wavelet based forecasting of returns is more effective for out-of-sample prediction, both at aggregate and across scales.

The structure of this paper is as follows: Section 2 reviews the literature, covering both theoretical and empirical perspectives on exchange rate properties and wavelet applications, with an emphasis on time-varying volatility, contagion, long memory, chaos, and forecasting. Section 3 outlines the data and methodology. The penultimate section presents the findings and discussion. Finally, Section 5 concludes the paper.

2. Literature Review

2.1.Theoretical Perspectives on the properties of exchange rates and Wavelet Multiscale Analysis

Volatility and long memory are interconnected nonlinear time series concepts crucial to understanding exchange rates. Volatile time series often exhibit long memory, where volatility shocks may persist over long periods (Cajueiro and Tabak, 2004; Grau-Carles, 2005). This may be due to the presence of nonlinear dynamics (Baruník et al., 2014). Long memory is characterized by autocorrelations that decay according to a power law, which further underscores its persistent behavior (Barkoulas et al., 2000; Mensi et al., 2019).Studies reveal that volatility can spread through contagion to other markets (King and Wadhwani, 1990), and relate to chaos via fractal patterns (Lahmiri et al., 2017)[11]. The presence or absence of these properties across scales captures market reactions to new information which may impact efficient price discovery, trade flows, investment decisions, and policy interventions. The following section reviews key studies aimed at modelling-time-varying volatility, identifying contagion, long memory, and chaos, and predicting exchange rates.

2.2.Modelling Time-Varying Volatility

A key feature of exchange rates is time-varying, clustered volatility, with long periods of elevated or muted turbulence punctuated by major jumps (Engle, 1982). Extensive research examines the

[11] Refers to price movements follow these self-similar, irregular patterns over time.

dynamics using models ranging from basic statistical measures to complex GARCH specifications (Martens, 2001; Bauwens and Sucarrat, 2010; Chortareas et al., 2007). Two main model classes capture observed clustering, leverage, and tail dependencies: conditional volatility as a function of observables, and stochastic volatility models with latent dynamics (Andersen and Bollerslev, 2018). Wavelets handle complications like non-stationarity and non-normality, enabling superior modelling of intricate, evolving volatility across frequencies (Ramsey and Zhang, 1996; Ramsey and Lampart, 1998; Jensen, 1999; In and Kim, 2013; Fernandez, 2005). Studies also highlight the ability of wavelets to identify structural breaks (Yazgan et al., 2015). Wavelets offer superior insights compared to standard GARCH or stochastic volatility models (Fernandez, 2008; Bekiros and Marcellino, 2013; Barunik et al., 2014; Gradojevic et al., 2020; He et al., 2023; Zivkov et al., 2021; Kuşkaya et al., 2022). Wavelets also outperform correlation methods by precisely localizing short-lived contagion episodes, offering better insights into temporary co-movements which are masked in standard time series models.

2.3.Contagion in Markets

Contagion refers to the cross-market transmission of shocks and volatility, challenging market efficiency by violating currency pair parity (Hernandez and Valdes, 2001; Dornbusch et al., 2000). Real and financial linkages enable spread through channels like trade and wealth effects, portfolio rebalancing, liquidity spirals, and bank lending exposures (Glick and Rose, 1999; Kaminsky and Reinhart, 2000). Theoretical modelling of contagion remains challenging but crucial for understanding currency interconnectedness (Aloui, 2011; Ahmad et al., 2013; Meng Huang, 2019; Shahrier et al., 2022;). Understanding long memory in returns is essential as it complements the study of contagion by highlighting how market shocks can have prolonged effects, challenging the assumption of rapid mean reversion in asset prices.

2.4.Capturing Long Memory in Returns

Exchange rates exhibit long memory, where past returns or volatility shocks show slow hyperbolic decay rather than the rapid exponential decay assumed in standard time series models (Baillie, 1996). This challenges the notion that markets efficiently incorporate new information. Theoretically, long memory relates to fractional integration, involving non-integer powers of the lag operator (Granger and Joyeux, 1980). Wavelet analysis uncovers long memory behavior across various horizons, often hidden in aggregated data. Studies confirm memory decreases at higher frequencies, supporting theories based on heterogeneous horizons (Jensen, 1999; Gençay et al., 2001). Notable research includes Teyssière and Abry (2007), Jensen and Witcher (2014), and Vo and Vo (2020).

2.5. *Investigating Chaos with wavelets*

Chaos, characterized by behavior that is highly sensitive to initial conditions within nonlinear deterministic systems, has become a significant focus in the analysis of financial time series (Chan and Tong, 2001; Mishra et al., 2011; Park and Whang, 2012; Bensaïda et al., 2015; Lahmiri, 2017; Vogl, 2022). Wavelets can isolate chaos at specific time scales, providing insights which are not evident from aggregate series. Bekiros and Marcellino (2013) using wavelet multiresolution analysis found that while wavelet decomposition techniques were effective in understanding the multiscale dynamics of currency markets, they did not conclusively prove chaotic behavior across all timescales in the forex market (Bekiros and Marcellino, 2013). Additionally, another study focusing on Moroccan exchange rates found that while chaotic structures were present in currency levels, they were not consistently observable in currency returns, highlighting the complexity and mixed results in detecting chaos (Lahmiri, 2017). These studies underline the challenges and varying outcomes when applying wavelet analysis to assess chaos in forex markets. Further, BenSaïda (2014) rejected noisy chaos at all frequencies for S&P 500 returns, while Lahmiri (2017) found evidence of chaos at the currency level but not in returns over 2009-2015. While there have been studies on chaotic dynamics in the Indian forex market, such as Sen and Chakrabarti (2014), who found that the chaotic nature of the INR-USD exchange rate limited the effectiveness of central bank interventions, and Datta and Bhattacharyya (2019), who identified fractal and chaotic behavior in major spot exchange rates, these studies do not explicitly examine chaos across different scales. Ahmad et al. (2017) also explored volatility spillovers in forex derivatives but did not focus on scale-specific analysis. Therefore, there remains significant scope for further research to investigate chaos dynamics in the Indian forex market from a multiscale perspective.

Building on the insights gained from studying chaos in financial time series with wavelet analysis, the next step is to explore how these complexities affect the prediction of exchange rates, where accurate forecasting becomes even more challenging.

2.6.*Exchange Rate Prediction*

Modeling and forecasting exchange rates present significant challenges due to high volatility, jumps, and complex nonlinear dynamics (Westerhoff, 2009). Conventional models like random walk, ARIMA, and GARCH have struggled to outperform simple naive forecasts (Rogoff and Stavrakeva, 2008), leading to interest in advanced techniques like wavelet analysis for better accuracy.

Exchange rate prediction is influenced by various factors including economic indicators, political developments, and investor sentiment, which contribute to the complexities and uncertainties of

financial markets(Froot and Rogoff, 1995). Frenkel (1979) highlighted forecasting difficulties in his monetary model, while Meese and Rogoff (1983) showed that random walk models outperformed structural ones, even when future explanatory variables were considered (Fair, 1986). Priewe (2017) found limited empirical support for neoclassical and new Keynesian theories. The efficient market hypothesis (EMH) suggests exchange rates incorporate all available information, making market outperformance challenging (Fama, 1970).

Accurate forecasting is crucial for managing risks and making informed decisions because it directly impacts the allocation of resources, asset pricing, and the mitigation of uncertainty. According to Rational Expectations Theory, economic agents make decisions based on forecasts that incorporate all available information, meaning that inaccurate forecasts can lead to suboptimal decisions, misallocation of capital, increased market volatility, and potential financial losses (Muth, 1961). Additionally, the Efficient Market Hypothesis (EMH) suggests that markets quickly incorporate new information, making it essential for participants to have accurate forecasts to remain competitive in rapidly changing environments (Fama, 1970). The literature on forecasting includes time series models (ARIMA (Box and Jenkins, 1976), VAR (Sims, 1980; Lütkepohl, 2005), exponential smoothing (Gardner, 1985)), structural models (DSGE (Lindé et al., 2016)), agent-based models (Fagiolo and Roventini, 2017), machine learning techniques (Hanke and Wichern, 2013), and judgmental approaches (Armstrong, 2001; Makridakis et al., 2010). Combining these methods can improve accuracy because each model captures different patterns and structures within the data. For instance, time series models are effective at capturing trends and cycles, structural models incorporate economic theory to explain underlying relationships, and machine learning techniques can detect complex, non-linear patterns. By integrating these diverse approaches, the combined model can better account for various sources of uncertainty and noise in the data, leading to more robust and reliable forecasts (Del Negro and Schorfheide, 2013).Wavelet analysis complements by decomposing time series into different frequencies (Gencay et al., 2001).

Early studies which accounted for the scale specific dynamics, have shown improvements in forecasting accuracy over the traditional benchmark random walk (Ramsey and Zhang, 1997; Kim and In, 2005). Recent studies integrating wavelets with machine learning show convincing results at short horizons (Mitra and Mitra, 2006; Dunis et al., 2010; Singhal and Swarup, 2011; Kilic and Ugur, 2023), but long term forecasts exhibit mixed results vis-à-vis the random walk. remains mixed (Hong and Lee, 2003; Andreou et al., 2013). Combining wavelets with machine learning may enhance forecasting outcomes. Theoretical motivation for this approach comes from the ability of wavelets to reduce noise and highlight relevant features, which machine learning models can then use more effectively to

produce forecasts that are both more accurate and resilient to the volatility inherent in financial markets.

Wavelets outperform traditional time series models in modelling complex exchange rate dynamics across different time horizons by effectively localizing nonlinearity and capturing both short-term fluctuations and long-term trends. They offer flexibility in capturing properties like time-varying volatility, interdependence, long memory, contagion, and nonlinear dynamics across time and frequencies. However, to the best of our knowledge the application of wavelet-based forex modelling in the Indian context remains limited.

This study aims to fill this gap by analyzing India's multiscale forex volatility dynamics over various time horizons and comparing wavelet-based forecasting approaches with traditional methods. The findings will provide comprehensive insights into forex market dynamics, benefiting policymakers, investors, and researchers by offering a less restrictive and more detailed understanding of risk management and market behavior. The next section details the methods used for analysis and justifies the choice of each approach.

3. Data and Methodology

3.1. Data

Our empirical analysis focuses on four major exchange rate pairs: the Indian Rupee (INR) against the US Dollar (USD), Euro (EUR), British Pound (GBP), and Japanese Yen (JPY), covering the period from January 6, 1999, to September 5, 2023. The data is sourced from the Reserve Bank of India's Database on Indian Economy (DBIE).The following figure 1 summarizes the methodological outline of the study.

Figure 1. Methodological Outline

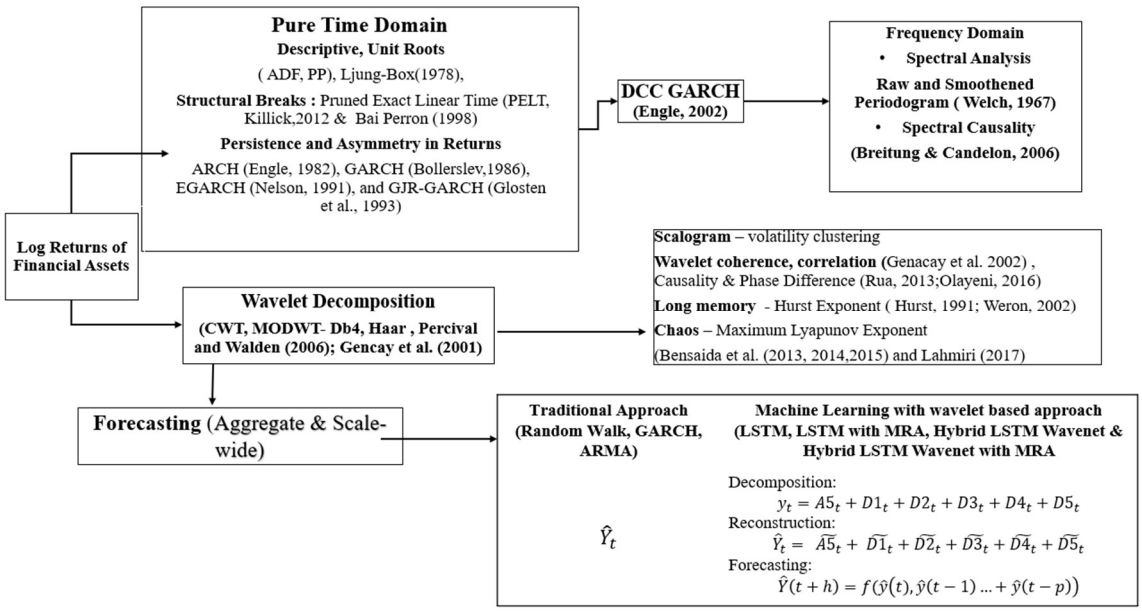

3.2. Methodology

The methodology of our study is structured into two key branches: one emphasizing a pure time domain-based approach, followed by a frequency domain perspective, and the other incorporating a wavelet-based approach augmented with non-linear methods to examine scale-wide properties and predict exchange rate returns.

First, we calculate the daily log-returns of the exchange rates.[12] Preliminary tests including unit root tests (Augmented Dickey-Fuller and Phillips-Perron), persistence test (Ljung-Box), and structural break tests (Pruned Exact Linear Time (PELT) algorithm, Kllick 2012) [13] are then conducted before estimating the volatility model. We then fit univariate volatility models, including ARCH (Engle, 1982), GARCH (Bollerslev, 1986), EGARCH (Nelson, 1991), and GJR-GARCH (Glosten et al., 1993), as a precursor to implementing a multivariate DCC-GARCH (Engle, 2002) model to assess persistence, asymmetry, and volatility spillovers[14]. The two-step estimation procedure here involves

[12] $[\ln(P_t) - \ln(P_{t-1}) * 100]$ where P_t is the exchange rate at a given time *t*.

[13] The PELT approach provides greater flexibility in identifying multiple changepoints in a time series compared to other structural break tests such as the Zivot-Andrews (1992); Gregory Hensen (1996); and Bai-Perron (1998)). Unlike some methods that rely solely on statistical data, our identification of changepoints also incorporated periods recognized in the literature as significant episodes of financial distress. This dual approach ensures a more comprehensive analysis. For a detailed explanation of the PELT algorithm, please refer to Killick (2012, p. 1592).

[14] A detailed exposition of each of these models can be found in (Tsay, 2002, pp.97-144 and Glosten et al., 1993, pp. 1782)

estimating the series of univariate GARCH model and then the correlations. The dynamic correlation structure is given as:

$$R_t = diag(Q_t^{-1/2}) Q_t diag(Q_t^{-1/2}) \quad (1)$$

$$Q_t = (1 - \alpha_n - \beta_n)\bar{Q} + \alpha_n(\varepsilon_{t-1}\varepsilon^T{}_{t-1}) + \beta_n Q_{t-1} \quad (2)$$

Where, R_t is the time varying conditional correlation matrix with all diagonal elements 1, α *and* β are the parameters that control conditional correlation and satisfy $0 \leq \lambda_1 + \lambda_2 < 1$. $\bar{Q} = cov[\varepsilon_t \varepsilon_t^T] = E[\varepsilon_t \varepsilon_t^T]$, $diag(Q_t)$ is an unconditional covariance matrix of standardized errors ε_t.

The estimated conditional correlations from DCC GARCH are then used to examine the presence of contagion effect following which an event based assessment is done to check whether strong correlations exist during the episodes of increased volatility and financial distress as identified by PELT method. Next, we perform a spectral analysis of the returns by examining raw and smoothened periodograms (Welch, 1967), defined as:

a) $$X[n] \underset{DFT;L}{\longleftrightarrow} X[k] \sim \frac{1}{L} |X[k]|^2 \quad (3)$$

Where $X[k]$ are the Discrete Fourier Transform (DFT) coefficients and then using a quantity proportional to the squared magnitude of DFT coefficients divided by L for n=0,1,…, L-1.The Welch estimate of Power Spectral Density ($\hat{S}_x^W(\omega_k)$) is given by :

b) $$\hat{S}_x^W(\omega_k) \triangleq \frac{1}{K} \sum_{m=0}^{K-1} P_{x_m}, M(\omega_k) \quad (4)$$

Where K is the number of segments into which signal is divided, $\sum_{m=0}^{K-1}$ is the sum overall K segments and $P_{x_m}, M(\omega_k)$ is the periodogram of m-th segment at frequency ω_k. We then conduct wavelet decomposition of each return series to investigate scale-wide properties[15]. This includes scalogram analysis using Continuous Wavelet Transform (CWT) which represents the intensity of different frequency components in a time series ,and is given as :

$$(s,t) = |CWT(x,s,t)|^2 \quad (5)$$

where x is the input time series, CWT(x,s,t) is the continuous wavelet transform of x at scale s and time t. $|.|^2$ is the magnitude squared of the CWT coefficients. In the next step, following Fernández-Macho (2012), we estimate wavelet coherence, correlation, and phase difference for Maximal Overlap

[15] For proof on the derivation of wavelet coefficients, refer to Appendix 12.A5, (Woodward et al. 2012 pp. 475-476)

Discrete Wavelet Transform (MODWT)[16] decomposed series using a Daubechies filter with four vanishing moments (db4)[17]. MODWT is translation invariant and provides a more asymptotically efficient wavelet variance estimator than DWT (Crowley, 2007;Barunik et al., 2014). These measures provide insights into interdependence, contagion, and cross-volatility spillovers (Genaçay et al., 2002; Rua, 2013; Olayeni, 2016). For a vector x of N observations, the MODWT can be described in terms of details and approximation coefficients as:

$$\widetilde{\mathbf{W}}_{\boldsymbol{J}} = \widetilde{\boldsymbol{W}}_{\boldsymbol{J}}\boldsymbol{X} \;\; and \;\; \widetilde{\mathbf{V}}_{\boldsymbol{J}} = \widetilde{\boldsymbol{V}}_{\boldsymbol{J}}\boldsymbol{X}, \tag{6}$$

Where $\widetilde{\mathbf{W}}_{\boldsymbol{J}}$ and $\widetilde{\mathbf{V}}_{\boldsymbol{J}}$ are the circularly shifted versions of jth level detail and approximation coefficients. In terms of additive decomposition, this can be expressed as:

$$X = \sum_{j=1}^{j_0}(\widetilde{\mathrm{D}_j})(\widetilde{\mathrm{S}_{J0}}) \text{ , for any } J_0 \geq 1 \tag{7}$$

Here, the scaling function of Daubechies wavelet with 4 vanishing moments (db4) is specified as $\varphi_t = \sum_{n=0}^{N-1} h_n\sqrt{2}\varphi(2t-n)$, where h_n are the scaling coefficients and n=4. The high-pass mother wavelet is given as $\psi_{\mathrm{t}} = \sum_{n=0}^{N-1}(-1)^n h_{N-1-n}\sqrt{2}\,\varphi(2t-n)$, where h_{N-1-n} is mirrored version of scaling coefficients.

Now, for a multivariate stochastic process $\mathrm{x_{1t}}, \mathrm{x_{2t}}\ldots\ldots\ldots\ldots, \mathrm{x_{nt}}$, assuming $\mathrm{W_{jt}} = (\mathrm{w_{1jt}}, \mathrm{w_{2jt}}, \ldots \mathrm{w_{njt}})$ as the detail coefficients corresponding to the scale λ_j obtained by applying MODWT to each $\mathrm{x_{it}}$ process (Gencay et al., 2002; Percival and Walden,2006). We can estimate variance, covariance, and cross-correlation using the MODWT coefficients for scale $\boldsymbol{\tau_j} = \mathbf{2}^{\boldsymbol{j-1}}$ as:

$$\text{Variance :} \qquad \hat{\sigma}_x^2(\tau_j) = \frac{1}{\widehat{N}_j}\sum_{k=L_j-1}^{N-1}(\widehat{W}_{j,k})^2 \tag{8}$$

Where $(\widehat{W}_{j,k})^2$ is the squared wavelet coefficient associated with scale j at data point $\mathrm{x_k}$. The covariance is given as :

$$\Upsilon_{XY}(\tau_j) = cov_{XY}(\tau_j) = \frac{1}{\widehat{N}_j}\sum_{k=L_j-1}^{N-1}(\widehat{W^x}_{j,k})(\widehat{W^y}_{j,k}) \tag{9}$$

The wavelet cross-correlation method breaks down the cross-correlation between two time series on a scale-by-scale basis, enabling an examination of how their relationship changes across different time horizons. Gençay, Selçuk, and Whitcher (2002) define the wavelet cross-correlation as:

[16] The choice of different transforms and filters considers the properties of interest to be examined. Key considerations include ensuring orthogonality, optimal localization of both fast and slow transitions in the time series, effective capture of slow transitions, and vanishing moments to represent polynomial trends or components of a time series accurately.For detailed explanation see Percival and Walden (2006, pp. 168-173)

[17] For detailed explanation on the choice of mother wavelet, refer to appendix 2, section 2.1

$$\widehat{\rho_{XY}}(\tau_j) = \frac{cov_{XY}(\tau_j)}{\hat{\sigma}_X^2(\tau_j)\hat{\sigma}_Y^2(\tau_j)}$$

Or $$\widehat{\rho_{x,k}}(\tau_j) = \frac{\Upsilon_{x,k}(\tau_j)}{\widehat{\sigma_1}(\tau_j)\hat{\sigma}_2^2(\tau_j)} \quad (10)$$

where $\hat{\boldsymbol{\sigma}}_{\boldsymbol{x,k}}^{\boldsymbol{2}}(\boldsymbol{\tau_j})$, $\boldsymbol{\sigma^2(\tau_j)}$ are the wavelet variances for $\boldsymbol{x_{1,t}}$ and $\boldsymbol{x_{2,t}}$ associated with scale $\boldsymbol{\tau_j}$ and $\boldsymbol{\Upsilon_{XY}(\tau_j)}$ respectively, and the wavelet covariance between $\boldsymbol{x_{1,t}}$ and $\boldsymbol{x_{2,t-k}}$ associated with $\boldsymbol{\tau_j}$. The wavelet cross-correlation is employed to identify the lead-lag relationship between two time series on a scale-by-scale basis. Finally, Olayeni (2016) proposed an alternative to the Discrete Wavelet Transform (DWT) for assessing Granger Causality, using the Continuous Wavelet Transform (CWT) based correlation measure developed by Rua (2013). It is expressed as follows:

$$G_{Y\to X}(s,\tau) = \frac{\xi\{s^{-1}|\mathbb{R}\big(W_{XY}^m(s,\tau)\big)I_{Y\to X}(s,\tau)|\}}{\xi\left\{s^{-1}\sqrt{|W_x^m(s,\tau)|^2}\right\}.\xi\{s^{-1}\sqrt{|W_y^m(s,\tau)|^2}\}} \quad (11)$$

Where $W_X^m(s,\tau)$, $W_Y^m(s,\tau)$and $W_{XY}^m(s,\tau)$ are the wavelet transformations and

$$I_{Y\to X}(s,\tau)\begin{cases}1 & if\ \varphi_{XY}(s,\tau)\epsilon\ \left(0,\frac{\pi}{2}\right)U\ (-\pi,-\frac{\pi}{2}) \\ 0 & otherwise\end{cases} \quad (12)$$

and phase difference is given as:

$$\varphi_{XY}(s,\tau) = tan^{-1}\left(\frac{\xi\{W_{XY}^m(s,\tau)\}}{\mathbb{R}\{W_{XY}^m(s,\tau)\}}\right) \quad (13)$$

The decision criterion for a bivariate process is based on phase angle conditions as illustrated in Figure 3. An arrow pointing right implies zero phase difference, indicating synchronized movements and positive correlation. An arrow pointing left indicates a 180° phase difference, showing negative correlation. Upward and downward arrows represent phase differences of π/2 and -π/2, indicating that one variable leads the other. Phase angles $\varphi_{XY}\ \epsilon\left(0,\frac{\pi}{2}\right)$ or $\left(-\pi,-\frac{\pi}{2}\right)$ show that the second variable is leading first, whereas $\varphi_{XY}\ \epsilon\left(-\frac{\pi}{2},0\right)$ or $\varphi_{XY}\ \epsilon\left(\frac{\pi}{2},\pi\right)$ represents the first variable leading the second.

Fig.3. Phase angle conditions

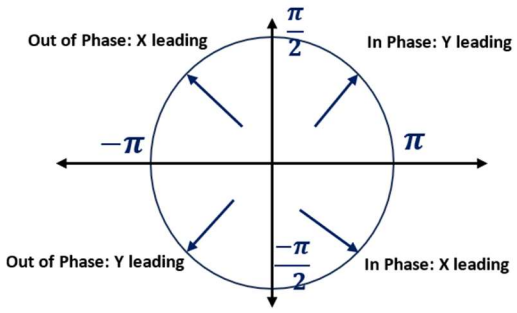

Source: Firouzi and Wang (2020)

Further, we test for causal dynamics in the frequency domain for each aggregate exchange rate return series, details, approximation coefficients based on Breitung-Candelon (2006) Spectral Granger causality test following Ronderos (2016, pp.2). For y_t does not cause x_t at a specific frequency ω. The measure is given as :

$$M_{y\to x}(\omega) = \log\left[1 + \left[\frac{|\psi_{12}(e^{-i}\ )|^2}{|\psi_{11}(e^{-i}\ )|^2}\right]\right] \tag{14}$$

$where\ \psi_{11}(e^{-i\omega})\ and\ |\psi_{12}(e^{-i\omega})|$ are elements of transfer function matrix $\psi(L) = \ominus\ (L)^{-1}G$ in the frequency domain, where $\ominus$(L) is a matrix of polynomial in lag operator L and G is lower triangular matrix from Cholesky decomposition of covariance matrix of errors. $|\psi_{12}(e^{-i\omega})| = 0$ implies that y_t does not cause x_t at frequency ω. The null hypothesis for test is :

$$H_0: R(\omega)\beta = 0$$

Where $\beta = [\Theta_{12,1}, \Theta_{12,2}, \dots, \Theta_{12,p}]$ is the coefficient vector and $R(\omega)$ is the sine cosine matrix of restrictions based on frequency ω.

In order to test for long memory test, the classical and corrected Hurst exponent (Hurst, 1951), and sample-adjusted approach the Anis-Loyd corrected Hurst exponent (H*)(Weron, 2002) which use rescaled range analysis (R/S) (Mandelbrot and Wallis, 1969) are conducted. These are given as :

$$\frac{R_n}{s_n} = C * n^H \tag{15}$$

Where, R_n is the adjusted range, s_n is the standard deviation, n is the window size, and H is the Hurst exponent. $\frac{R_n}{s_n}$ is known as the rescaled range. Further, Anis-Loyd corrected Hurst exponent (H*) is estimated, which corrects the bias in H to estimate the true long-term scaling behavior better when dealing with real (finite) time series data. In equation form, it is given as:

$$\left(\frac{R}{S}\right)_{AL} = \frac{R_n}{s_n} - AL = \left(\frac{R}{S}\right)_n - E\left(\frac{R}{S}\right)_n + \sqrt{\frac{n\pi}{2}} \tag{16}$$

Where slope of $\left(\frac{R}{S}\right)_n$ vs Log-Log plot is the classic Hurst exponent and the slope of R/S-AL vs Log-Log plot is the AL corrected Hurst exponent. A Hurst exponent of 0.5 implies a random process, the value in the range $0.5 < H \leq 1$ confirms persistence and long memory in the series, and $0 \leq H < 0.5$ signifies an anti - persistent mean reversion behaviour.

Since the exchange rate returns were stationary at level, this approach is preferred over competing approaches like the detrended fluctuation analysis (DFA) and Geweke-Porter-Hudak (GPH) estimator, which is better suited for estimating Hurst exponent in non-stationary series by adjusting it for linear

trends. Further, the rescaled range analysis does not require the assumption of Gaussianity (Mandelbrot and Wallis, 1969) which is advantageous over competing approaches (Granero et al., 2008).

Next, in order to examine sensitivity to initial conditions, we examine the presence of chaos by estimating the maximum Lyapunov exponent at each scale for all exchange rate returns based on Nyschka et al. (1997); Bensaïda et al. (2013); Bensaïda (2014, 2015)[18].

Finally, to assess the forecast accuracy of exchange rates, we compare forecast errors of Random Walk, ARIMA, GARCH, and Hybrid Wavelet-LSTM models of both aggregate and scale-specific return series. We use the standard measures of Root Mean Square Error (RMSE) and Mean Absolute Error (MAE) as metrics. Scale-dependent RMSE and MAE comparisons help determine optimal methods for different time horizons. Wavelet domain errors can be aggregated to the time domain using inverse MODWT to examine overall forecast accuracy (Tan et al., 2010). Following Kılıç and Ugur (2023), we estimate a simple LSTM and Hybrid Wavelet-LSTM models (i.e., LSTM with MRA, Hybrid LSTM - Wavenet and hybrid LSTM Wavenet with MRA) using polynomial powers of sigmoid as the activation function[19]. The forecast error comparisons are made across all models both at aggregate levels and across scales. The generic form of the models we have estimated are given below[20]:

a. Random Walk : $y_t = y_{t-1} + u_t$
b. ARMA : $\widehat{y_t} = \varphi_1 y_{t-1} + \cdots + \varphi_p y_{t-p} + \theta_1 \epsilon_{t-1} + \cdots + \theta_q \epsilon_{t-q} + \epsilon_t$
c. GARCH : $\sigma_t^2 = \alpha_0 + \alpha_1 \varepsilon_{t-1}^2 + \beta_1 \sigma_{t-1}^2$
d. Hybrid LSTM- Wavenet :

The basic structure of LSTM Model[21] is given as :

$$\text{Forget Gate : } \mathrm{F_t} = \sigma(\mathrm{W_F x_t} + \mathrm{U_F h_{t-1}} + \mathrm{b_F}) \quad (17.1)$$

$$\text{Input Gate : } \mathrm{I_t} = \sigma(\mathrm{W_I x_t} + \mathrm{U_I h_{t-1}} + \mathrm{b_I}) \quad (17.2)$$

[18] Refer to appendix 1 provides a detailed explanation on chaos identification process

[19] In WaveNet models, fixed translation and dilation parameters during initialization are crucial. Overly small parameters should be avoided due to the quickly vanishing nature of wavelets (Wen et al., 2009). To address this, we initialized the parameters as $u_i = \frac{0.5(\beta-\alpha)}{n}$, $v_i = \frac{0.5(\beta+\alpha)}{n}$, where n is the number of LSTM nodes, and α and β are the minimum and maximum values in the training set. Each activation function was produced using the formula:

$$\Psi_6^j(x) = \frac{\Psi(\mathrm{x} - u_i * j)}{v_i} * j$$

where j is the index of activation functions. This means that for each level j, the function is scaled and shifted based on the parameters u_i and v_i times *j*. The wavelets considered in the estimation were based on their ability to capture return behavior and localization, which include: db2, db4, db8, sym2, sym4, sym8, coif1, coif2, haar, bior1.3, bior3.5, and bior6. To enhance model fit, Talos optimization was used to identify parameters that improve the observed error metrics (MAE and RMSE).

[20] The optimal models estimated under each category are explained in results section 4.10.

[21] Refer to Olah (2022), for detailed explanation on LSTM network.

$$\text{Candidate State} : \tilde{C}_t = \tanh\left(W_C x_t + U_C h_{t-1} + b_c\right) \quad (17.3)$$

$$\text{Cell State} : C_t = F_t \odot C_{t-1} + I_t \odot \tilde{C}_t \quad (17.4)$$

$$\text{Output Gate} : O_t = \sigma(W_o y_t + U_F h_{t-1} + b_o) \quad (17.5)$$

$$\text{Output} : h_t = F_t \odot \tanh\left(C_t\right) \quad (17.6)$$[22]

The following section presents the analysis and discussion of results.

4. Empirical Results and Discussion

4.1. Descriptive Statistics

The descriptive statistics summarized in Table 1 below show significant variability in exchange rates with high skewness and kurtosis. INRUSD and INRGBP exhibit negative minimum values, indicating potential extreme drops. Jarque-Bera test probabilities suggest non-normal distribution for all pairs. The deviations in returns point to macroeconomic differences, policy divergence, and individual market structures influencing participant behaviors[23].

Table. 1. Descriptive Statistics – Returns

	INRUSD	INREUR	INRGBP	INRJPY
Mean	0.011	0.0097	0.006	0.008
Median	0.000	0.004	0.014	0.000
Maximum	4.012	4.155	3.679	5.764
Minimum	-3.006	-3.889	-6.775	-5.123
Std. Dev.	0.397	0.626	0.620	0.762
Skewness	0.202	0.050	-0.564	0.252
Kurtosis	10.828	5.484	9.790	6.848
Jarque-Bera	14949.590	1504.2	11526.64	3663.9
Probability	0.000000	0.000	0.000	0.000
Sum	66.744	56.3851	35.142	50.648
Sum Sq. Dev.	918.400	2291.312	2247.337	3386.023
Observations	5839	5839	5839	5839

The unit root test results in Table 3 in Appendix 3 show that all the variables were stationary after taking their log returns at a 5 percent level of significance. The Ljung-Box Statistic results for serial

[22] At each time step t, the LSTM unit processes an input vector x_t, using the input weight matrix W and combines it with the previous output h_{t-1} using the recurrent weight matrix U. A bias vector b is added. The activation of the forget gate F_t at time t determines the information that will be discarded from the cell state. The input gate I_t regulates the new information to be added. The candidate state vector at time ($\tilde{C}_t$) represents a combination of the current input and previous state information. The cell state C_t is updated based on the input and forget gates.

The output gate O_t controls the final output (h_t) derived from the cell state. The polynomial power of sigmoid which is used as a wavelet activation function in the Hybrid model is specified as :

$$\text{PPS } \psi_n(y) = \sum_k^n \sum_{j=0}^k (-1)^j (j+1)^n \binom{k}{j} f^{k+1}(y) \quad (18)$$

[23] The plots for raw data, returns, distribution, and correlations are presented in Appendix 3 - Fig.2.a-b., and Table 2 respectively.

dependence of residuals indicate persistence and volatility clustering in exchange rate returns, as they lead to the rejection of the null hypothesis. This is supported by p values for all variables being below 0.05, signifying a 5 percent level of significance (refer to Table 4, Appendix 3). Consequently, it is evident that not all autocorrelations up to lag 10 are zero, thus confirming the presence of volatility clustering in the residual series. Further, autocovariances in the squared returns are persisting up to approximately lag 20 for each of the currency pairs (Figure 3., Appendix 3).

Based on the structural break identification using PELT algorithm, among the identified breakpoints, the study considers breakpoints that align with the more pronounced financial distress events in the forex markets literature. The entire period of study is classified under two scenarios; a) Financial distress which encompasses Asian Financial Crisis and Dot com Bubble (1997 - 2001), GFC (2007-2009), Eurozone Debt Crisis (2010 - Apr2011), Taper Tantrum (2013), Brexit (June 2016-2017), COVID-19 and Russia Ukraine War (2020-2023), and b) the regular periods: Pre GFC (2003-2006), Post GFC (2009-2015) and 2015-2020[24].

4.2. DCC-GARCH Estimation Results

Table.7. Estimation Results - DCC GARCH

Optimal parameters	Estimate	Std. Error	t value	Pr(>|t|)
$\mu_{ZINRUSD}$	-0.001	0.002	-0.26	0.796
$\omega_{ZINRUSD}$	0.001	0.000	2.19	0.028
$\alpha 1_{ZINRUSD}$	0.146***	0.018	8.18	0
$\beta 1_{ZINRUSD}$	0.853***	0.019	43.61	0
$\mu_{ZINREUR}$	0.006	0.007	0.86	0.388
$\omega_{ZINREUR}$	0.003	0.001	2.33	0.02
$\alpha 1_{ZINREUR}$	0.047***	0.001	4.83	0
$\beta 1_{ZINREURr}$	0.944***	0.013	74.06	0
$\mu_{ZINRGBP}$	0.005	0.007	0.70	0.482
$\omega_{ZINRGBP}$	0.009	0.003	3.00	0.003
$\alpha 1_{ZINRGBP}$	0.061***	0.013	4.59	0
$\beta 1_{ZINRGBP}$	0.914	0.019	48.11	0
$\mu_{ZINRJPY}$	-0.003	0.009	-0.39	0.69
$\omega_{ZINRJPY}$	0.015	0.005	2.98	0.003
$\alpha 1_{ZINRJPY}$	0.086***	0.013	6.78	0
$\beta 1_{ZINRJPY}$	0.889***	0.018	49.16	0
[Joint]dcca1	0.026***	0.003	8.15	0
[Joint]dccb1	0.966***	0.004	214.39	0
Information Criteria				
Akaike	4.7805			
Bayes	4.808			
Shibata	4.7805			
Hannan-Quinn	4.7901			

Note: ***, **, * denotes 1, 5, and 10 - percent level of significance, respectively

[24] Figure 4 and Table 6. In Appendix 4 summarize the identified break periods.

Table 7 reports the estimation output of the DCC GARCH model. Significant ARCH (α_i) and GARCH (β_i) effects are observed across all variables at the 5% level. The significant DCC coefficients ($joint\ \alpha_i\ and\ \ joint\beta_i$) indicate short-term spillover and long-term persistence of INRUSD returns on other exchange rates. The sum of DCC coefficients being less than 1 confirms dynamic conditional correlations.

The estimated conditional correlations depicted in Figure 5.a. (Appendix 4.2.) demonstrate both positive and negative linkages across all currency pairs. During periods of financial distress, negative or low correlations suggest a flight to safety due to uncertainty. Conversely, higher correlations during these periods indicate a risk-on or risk-off environment, where market participants view return pairs as risky assets that exhibit comovement.

The conditional covariance in exchange rate returns (Figure 5.b., Appendix 4.2) illustrates volatility spillovers among exchange rate variables. Higher covariances indicate increased interdependence, particularly during financial crises like the Global Financial Crisis, the FED Taper in 2013, and the COVID-19 pandemic. Notably, USDJPY and EURJPY pairs exhibit significant volatility spillovers. Positive covariance during crises suggests increased market interdependence, emphasizing the need for diversification. Negative or low covariance in other pairs indicates independent movement, highlighting potential diversification benefits in portfolios. This underscores the importance of strategic portfolio balancing to mitigate risk during financial distress. These findings align with Adrian et.al. (2024), who highlight that emerging markets experience varying degrees of currency depreciation driven by interest rate differentials with the US, impacting financial stability during periods of global uncertainty.

4.3.Contagion

To have preliminary insights on the presence of the contagion effect[25] , we assess whether strong correlations exist during the episodes of increased volatility and financial distress based on estimated conditional correlations from DCC - GARCH.

Table 8. Pre and post Crisis conditional correlation – intra (forex) and inter-market returns

	Events	USD-EUR*	USD-GBP	USD-JPY	GBP-EUR	GBP-JPY	EUR-JPY
Financial Distress Events	Asian Financial Crisis and Dot com Bubble (1997 - 2001)	0.157	0.223	0.229	0.604	0.182	0.156
	GFC (2007-2009)	0.322	0.297	0.583	0.654	0.229	0.411

[25] Here we define contagion in terms of financial distress and volatility transmission from one asset to another, resulting in increased correlations(Pindyck and Rotemberg (1993); Karolyi and Stulz (1996) Masson (1998), Chiang et al. (2007);;Siedlecki and Papla(2016).

	Eurozone Debt Crisis(2010 - Apr 2011)	0.09	0.267	0.547	0.506	0.24	0.263
	Taper Tantrum (2013)	0.579	0.594	0.463	0.78	0.564	0.515
	Brexit (June 2016-2017)	-0.049	-0.061	0.174	0.443	-0.063	0.442
	COVID-19 and Russia Ukraine War (2020-2023)	0.282	0.135	0.406	0.589	0.303	0.465
Normal Period	Pre GFC (2003-2006)	0.065	0.118	0.13	0.716	0.419	0.441
	Post GFC (2009-2015)	0.212	0.346	0.589	0.583	0.296	0.301
	2015-2020	0.276	0.239	0.418	0.577	0.29	0.493

Notes: * USD-EUR refers to dynamic conditional correlation and covariance of INRUSD returns against INREUR returns, and likewise
for the other currency pairs respectively

The results in table 8 show that correlations generally increase during crises compared to normal periods, signifying higher interdependence. For example, the USD - EUR correlation increased from 0.065 pre-GFC to 0.322 during GFC, pointing to contagion. Covariances also spike in crises, signifying greater simultaneous movements and spillovers between pairs. USD-JPY covariance jumped from 0.020 pre-GFC to 0.431 during GFC, highlighting market turmoil. The Eurozone Debt Crisis shows a high USD-JPY correlation but lower EUR correlations, indicating contained contagion. Brexit caused a negative USD-EUR correlation due to flight-to-safety effects. The COVID-19 crisis shows more moderate correlations and spillovers than the GFC, possibly due to timely policy interventions. The Taper Tantrum period (2013) stands out with exceptionally high covariances across all pairs due to Fed policy shocks. Overall, the DCC-GARCH results demonstrate significant increases in interdependence during crisis events compared to calmer periods, revealing the extent of spillovers.

4.4.Variance Analysis : Spectral and Wavelet Decomposition

We estimated the spectral content of returns series using the raw periodogram and the smoothed Welch periodogram to reduce leakage (Figure 6, Appendix 4). The x-axis, spanning from 0 to 0.5 (Nyquist frequency), indicates long-term patterns near 0 cycles per day to shorter patterns around 2 days. Peaks in power highlight high variation events and dominant frequencies, with a notable cyclical pattern around a frequency of 0.2, indicating periodicity every 5 days. The next section provides time-frequency decomposition results for a more detailed analysis of exchange rate return dynamics.

Table 9 in Appendix 4 summarizes power spectrum variations across financial distress and normalcy periods, showing that the Taper Tantrum episode had the highest exchange rate return fluctuations, followed by the GFC, Brexit, and the Eurozone crisis. Periods of normalcy exhibited lower volatility, confirming that crises lead to higher volatility. These findings align with the DCC-GARCH contagion analysis, which revealed increased correlations and covariances during crises.

4.5.Multiscale Volatility Dynamics

Figure 7.a. below presents the scale-wide variance for the respective bilateral exchange rate pair obtained after the MODWT decomposition[26]. It is evident that within the first two days, the maximum variation in the exchange rate is explained at scale 1. Further, the INRUSD exhibits the least variation compared to the INREUR and INRGBP, while the INRJPY pair exhibits the highest variation across all scales.

Figure 7.a. Scale-wide variance in exchange rate returns

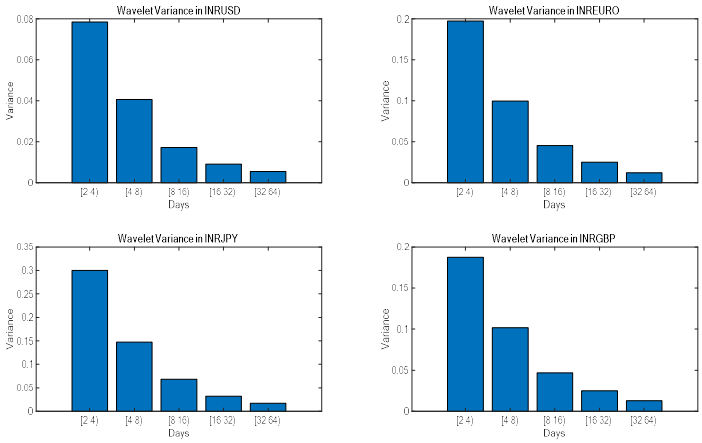

4.6.Crises Specific variance across scale in the currency market

The Figure 8.a.- e (Appendix 4.3., summarizes the scale-wide volatility in returns specific to periods of financial distress, i.e., the GFC(Aug 2007 – Aug 2009), the Eurozone (Jan 2010 – Apr 2011), Taper Tantrum (May 2013 – Sept 2013), Brexit (Jun 2006 – Dec 2007), and the COVID-19 (Jan 2020- Dec 2022). The MODWT variation across scales in pre, during, and post-crisis periods indicates a market-wide contagion effect with maximum variation exhibited at level 1 details, i.e., within two days intervals. In comparison, the most severe event has been the FED Taper talk, followed by GFC, COVID-19, Eurozone, and Brexit, respectively. Interestingly, the volatility of the post-pandemic returns showed more significant variation as compared to pre-pandemic levels, especially in the case of INREUR and INRJPY; on the contrary, for all other events, post crises levels accounted for a fall in the variance of returns.

4.7. Co-movements and Lead-Lag relationship: Wavelet Coherence and Phase Difference

Figure 9 shows the wavelet coherence between bilateral exchange rate return pairs, indicating lead-lag relationships during various financial periods. We consider the sampling interval of 1/265 of a year (in days) to display the periods in years. The phase shifts here are based on coherence values greater than

[26] Figure 7.b. in Appendix 3, section 3.3. presents the decomposition results for all the returns series

the specified phase display threshold of 0.6 In each subplot of the figure, there's a dashed white line and grey shaded areas extending from this line to the period and time axes, known as the cone of influence. This area indicates where the scalogram might be affected by edge-effect artefacts, which occur when wavelets stretch beyond the data's observation interval. The information within the cone, especially in the unshaded region enclosed by the white line, is considered a reliable representation of time-frequency data. However, the data in the shaded areas outside the white line is viewed with caution due to potential edge effects.

Figure 9. Phase shift plots based on wavelet coherence for exchange rate returns

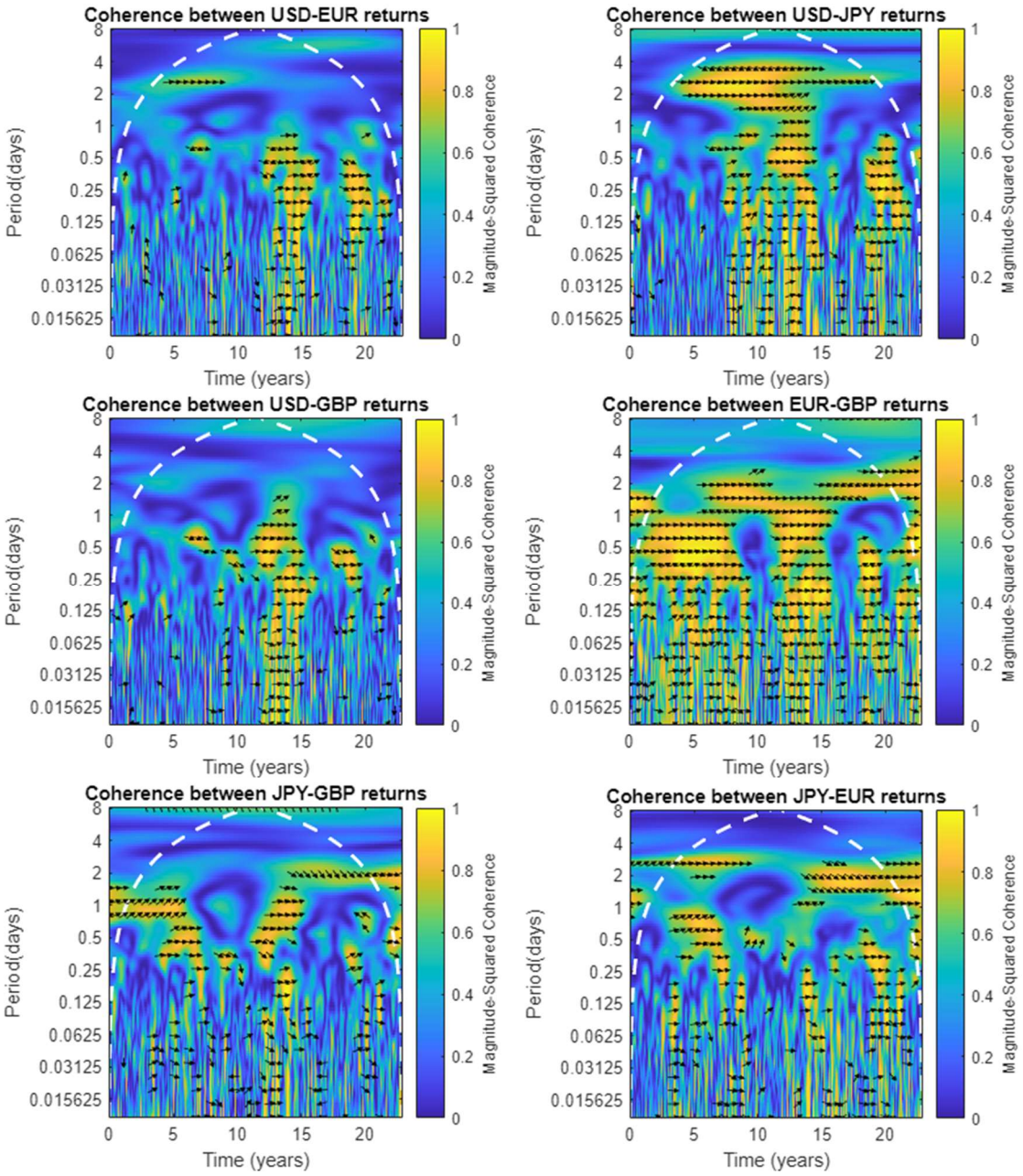

For INRUSD-INREUR, coherence varied with INRUSD leading until 2004-05, showing in-phase relationships during the GFC (2007), and leading again during the 2013 Fed taper talk. During COVID-19, INREUR initially led but eventually followed INRUSD. The highest coherence occurred during the Fed taper talk, reflecting significant market interdependence. The INRUSD-INRJPY pair exhibited strong coherence during the GFC, Fed taper talk, and COVID-19, with INRJPY consistently following INRUSD.

The INRUSD-INRGBP pair displayed similar patterns to INRUSD-INREUR, with strong coherence during the GFC and post-Brexit periods, though lower during the pandemic. INREUR-INRJPY showed INRJPY following INREUR with limited impact from the Fed taper talk, while INREUR-INRGBP had strong co-movement throughout. The INRJPY-INRGBP pair demonstrated significant correlations during financial distress.

All currency and cross-market return pairs exhibited significant co-movement during periods of financial distress, indicating increased interconnectedness and exposure to contagion effects. Notably, INRUSD led all other currency pairs over the long horizon, emphasizing its dominant role[27]. These findings underscore the vulnerability of global currency markets to contagion during crises, necessitating coordinated policy approaches and robust risk management strategies to mitigate systemic risks. Stakeholders must consider spillover effects and not view currency markets in isolation, particularly during financial stress periods. Understanding these linkages can aid in developing effective hedging strategies and regulatory measures to stabilize markets and prevent contagion from escalating.

4.7.1. Wavelet Cross-correlations and Phase Difference Across Scales

Figure 10 presents the cross-correlation sequence and 95% confidence intervals between INRUSD and other exchange rates. The wavelet cross-correlation sequence, particularly at the 2-4 day cycle scale, reveals significant insights. A peak negative correlation is observed at a one-day lag for all currency pairs, indicating that INRUSD consistently leads the other exchange rates by one day. Across all scales, a positive correlation exists between INRUSD returns and the returns of other exchange rate pairs, emphasizing the dominant role of INRUSD in leading exchange rate movements. This finding underpins the interconnectedness and influence of INRUSD on other currencies, highlighting the importance of monitoring INRUSD for anticipating changes in other exchange rates.

[27] The findings of scale-wide frequency domain causality test also support the wavelet coherence findings, and are summarized in Table 10 of appendix 4

Fig.10. Wavelet cross-correlations and Phase difference

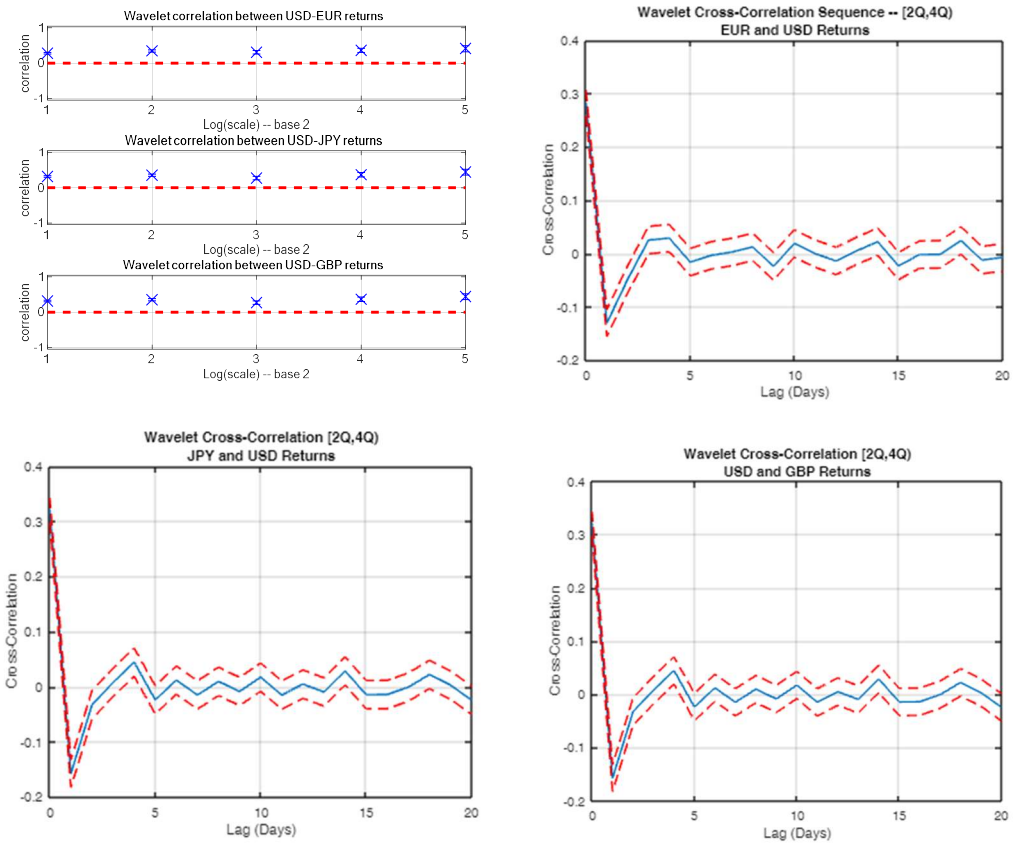

4.8.Multiscale Long Memory

The Hurst exponent estimates in Table 11. below indicates long memory at the aggregate level, while decomposed levels across different scales exhibit mean-reverting behaviour. At broader scales, influenced by market fundamentals, the Hurst exponent values exceed 0.5, suggesting persistence and long-term memory. This persistence in aggregate series and approximation coefficients aligns with macroeconomic fundamentals driving equilibrium exchange rates over the long run.

Table 11. Long Memory Estimation Results

Scales	Classical Hurst	Corrected Hurst	Decision	**Scales**	Classical Hurst	Corrected Hurst	Decision
INRUSDR	0.579	0.552	Long Memory	INRJPY	0.493	0.467	Near Random Process
D11	0.232	0.191	Mean reversion	D31	0.233	0.190	Mean reversion
D12	0.238	0.21	Mean reversion	D32	0.221	0.193	Mean reversion
D13	0.239	0.221	Mean reversion	D33	0.221	0.204	Mean reversion
D14	0.280	0.268	Mean reversion	D34	0.200	0.190	Mean reversion
D15	0.268	0.261	Mean reversion	D35	0.190	0.184	Mean reversion
A1	0.682	0.673	Long Memory	A3	0.662	0.652	Long Memory
INREUR	0.534	0.508	Long Memory	INRGBP	0.496	0.471	Near Random Process
D21	0.192	0.155	Mean reversion	D41	0.240	0.196	Mean reversion
D22	0.201	0.175	Mean reversion	D42	0.263	0.230	Mean reversion
D23	0.165	0.151	Mean reversion	D43	0.242	0.224	Mean reversion
D24	0.175	0.166	Mean reversion	D44	0.2261	0.215	Mean reversion
D25	0.226	0.22	Mean reversion	D45	0.224	0.217	Mean reversion

A2	0.663	0.654	Long Memory	A4	0.631	0.622	Long Memory

Note:D_{ij} and Ai implies the detail and approximation coefficients for corresponding return series up to j decomposition levels. Here, i=1 to 4 such that 1,2,3,4 implies INRUSD, INREUR, INRJPY and INRGBP returns.

Conversely, finer scales dominated by short-term market movements show Hurst exponent values below 0.5, indicating mean-reverting behaviour. This shift towards randomness at higher frequencies highlights the influence of transient market inefficiencies such as market microstructure effects, noise trading, liquidity fluctuations, seasonal patterns, policy interventions, and dynamic arbitrage activities. These factors contribute to short-term fluctuations, making them appear more random and less predictable.

For example, the INRUSD pair exhibits long memory at the aggregate level (Hurst exponent: 0.5793 classical, 0.552 corrected) but mean-reverting behaviour at finer scales (D11 to D15). Similarly, INREUR shows long memory at the aggregate level but mean reversion at finer scales (D21 to D25). This pattern is consistent across other pairs like INRJPY and INRGBP, where aggregate series show long memory, while decomposed levels indicate mean reversion.

4.9.*Multiscale chaos dynamics*

Table 12. Estimated Lyapunov exponents for Indian Exchange Rates using MODWT

	Sigmoid function		Tanh function	
	Lyapunov	Conclusion	Lyapunov	Conclusion
INRUSDR	-0.23***	No Chaos	-0.20***	No Chaos
A1	0.07	Chaos Exists	0.1	Chaos Exists
D11	-0.08***	No Chaos	-0.09***	No Chaos
D12	0	No Chaos	0.13	Chaos Exists
D13	0.1	Chaos Exists	0.16	Chaos Exists
D14	0.2	Chaos Exists	0.1	Chaos Exists
D15	0.04	Chaos Exists	0.15	Chaos Exists
INREUR	-0.25***	No Chaos	-0.17***	No Chaos
A2	0.05	Chaos Exists	0.07	Chaos Exists
D21	-0.03***	No Chaos	-0.07***	No Chaos
D22	0.08	Chaos Exists	0	No Chaos
D23	0.03	Chaos Exists	0.12	Chaos Exists
D24	0.08	Chaos Exists	0.02	Chaos Exists
D25	0.15	Chaos Exists	0.37	Chaos Exists
INRJPY	-0.19***	No Chaos	-0.21***	No Chaos
A3	0.11	Chaos Exists	0.03	Chaos Exists
D31	-0.05***	No Chaos	-0.06***	No Chaos
D32	0.01	Chaos Exists	0.02	Chaos Exists
D33	0.03	Chaos Exists	0.08	Chaos Exists
D34	0.04	Chaos Exists	0.22	Chaos Exists
D35	0.18	Chaos Exists	0.18	Chaos Exists
INRGBP	-0.23***	No Chaos	-0.21***	No Chaos
A4	0.11	Chaos Exists	0.03	Chaos Exists
D41	-0.06***	No Chaos	-0.04***	No Chaos
D42	-0.02***	No Chaos	0.13	Chaos Exists
D43	0.05	Chaos Exists	0.12	Chaos Exists
D44	0.12	Chaos Exists	0.21	Chaos Exists
D45	0.15	Chaos Exists	0.15	Chaos Exists

Note: The negative value here indicates the stability or convergence, i.e., the absence of chaos in the exchange rate. Dij implies the detail coefficients for INRUSD, INREUR, INRYEN & INRGBP returns respectively. Ai is the approximation coefficient for i=1 to 4 such that 1,2,3,4 implies INRUSD, INREUR, INRJPY and INRGBP returns.

Table 12 presents the results of scale-wise chaos identification in daily exchange rate returns using sigmoid and tanh activation functions, based on Lahmiri (2017). The largest Lyapunov exponents are predominantly negative and significant for both long and short movements, indicating the absence of chaos and a stable market. While some approximation coefficients show positive exponents, they lack consistent significance. These findings align with Lahmiri (2017) and suggest that exchange rate returns are mean-reverting and influenced by noise trading, order flow imbalances, and short-term macroeconomic events. In the Indian context, factors such as capital controls, RBI interventions, and strict capital flow monitoring contribute to the observed exchange rate stability.

A two-sample Kolmogorov-Smirnov test (K-S Statistic = 0.25, p-value = 0.30) revealed no significant difference in Lyapunov exponent distributions between the two activation functions, further reinforcing the stability of exchange rate returns driven by predictable macroeconomic factors. This absence of chaos implies that exchange rate returns in India reflect available information efficiently, minimizing extreme volatility and enhancing the reliability of the price discovery process. As a result, returns adjust predictably to new information, reflecting underlying economic conditions, though short-term inefficiencies due to speculative trading may still arise.

These insights can inform improved forecasting models for exchange rate movements and support better risk management and policy formulation in the Indian forex market.

4.10. Multiscale Forecasting

i) Scale wide comparison

Table 13 below summarizes the best performing forecast models across scales based on prediction error metrics[28]. Forecasting results indicate that the RMSE and MAE consistently decrease across different detail levels (D1 to D5) for all exchange rates, suggesting that higher decomposition levels yield more accurate forecasts compared to aggregate levels.

13. Best-Performing Models (RMSE)

Exchange Rate Returns	Best Model (Short-term, D1-D2)	Best Model (Mid-term, D3-D5)	Best Model (Long-term, Approximation)
INRUSD	Simple LSTM (D1)	ARMA (D2-D5)	ARMA (Approximation)
INREUR	Hybrid LSTM-Wavenet (D1-D5)	Hybrid LSTM-Wavenet (D5)	ARMA (Approximation)

[28] Refer to Forecasting results in Table 13.a for scale-wise details(Appendix 4, section 4.4)

INRJPY	Simple LSTM (D1-D4)	Hybrid LSTM-Wavenet (D5)	ARMA (Approximation)
INRGBP	Simple LSTM (D1-D4)	Hybrid LSTM-Wavenet (D5)	ARMA (Approximation)

Note: For each decomposition level 1000 Monte Carlo simulations were performed with a batch size of 1024 and 100 epochs.

The LSTM model performs relatively better in short-term (D1, 2-4 days) prediction, especially for INRGBP, while ARMA dominates long-term trends (D5, > 64 days) for stable currencies like INRUSD. Hybrid LSTM-Wavenet outperforms at mid-level scales (D2-D4, 4-32 days) and for volatile currencies like INREUR and INRJPY, highlighting the benefits of multiresolution analysis. This further bolsters the argument that model selection should depend on the forecast horizon, with machine learning models suited for short-term and ARMA for long-term trends.

14. Wavelet based machine learning forecast results for aggregate series of returns

Model	**INRUSD**		**INREUR**		**INRJPY**		**INRGBP**	
	RMSE	**MAE**	**RMSE**	**MAE**	**RMSE**	**MAE**	**RMSE**	**MAE**
GARCH	**0.216**[c]	0.172	**0.481**[d]	0.35	0.916	0.683	0.446[a]	0.34
ARMA	**0.21**[b]	0.162	0.481	0.351	0.919	0.688	0.447[c]	0.343
Random Walk	**0.209**[a]	0.161	**0.48**[c]	0.351	0.916	0.684	0.446[b]	0.34
LSTM - Test	0.299	0.22	0.**45**[b]	0.343	**0.568**[c]	0.624	0.585	0.422
LSTM + MRA – (db2)	**0.224**[d]	0.186	0.724	0.666	**0.864**[d]	0.839	0.692	0.639
LSTM Hybrid Wavenet	0.299	0.22	**0.449**[a]	0.342	**0.563**[b]	0.398	**0.568**[d]	0.404
Hybrid LSTM Wavenet with MRA- (db2)	2.34	2.32	2.784	2.76	2.507	2.476	6.457	6.441
LSTM + MRA – (sym8)	0.545	0.524	1.098	1.071	**0.354**[a]	0.3643	0.733	0.689
Hybrid LSTM Wavenet with MRA- (sym10)	4.608	4.607	4.09	4.081	6.639	6.624	5.807	5.788

Note : a, b, c and d are the ranked in ascending order of RMSE for each exchange rate pair. In each estimated LSTM model, the simulation exercise was carried out for 100 epochs with 1000 monte carlo simulations and then the average estimated error metrices were recorded for optimally identified mother wavelet from the considered set[29].

ii) Comparing traditional models with LSTM and Hybrid LSTM models with wavelet activation function

Table 14 presents the forecasting results for each return series, comparing traditional models, machine learning models, and machine learning models augmented with wavelet techniques. The table highlights the best-performing models after evaluating various mother wavelets. Figure 11 illustrates the ascending RMSE for these models, showing that traditional approaches like Random Walk,

[29] Refer to appendix 2, section 2.2. for details.

ARMA, and GARCH perform best for INRUSD and INRGBP returns, suggesting that these currency pairs are more stable and predictable. This stability is likely due to steady macroeconomic conditions and active interventions by the Reserve Bank of India (RBI). These results are consistent with the wavelet variance analysis, which also found INRUSD and INRGBP to be relatively stable.

In contrast, machine learning models, particularly wavelet-augmented LSTM, outperform traditional models for INRJPY returns, indicating the presence of complex, non-linear patterns and higher volatility. This volatility may be driven by speculative trading and external factors, such as Japan's economic policies. For INREUR, traditional models remain strong, but machine learning models like Hybrid Wavenet and simple LSTM also show competitive performance, suggesting some underlying complexities in this pair.

These findings suggest that the stability of India's forex market for major pairs like INRUSD and INRGBP is influenced by effective policy interventions, while the volatility in INRJPY and INREUR is likely due to external pressures and speculative forces. Consequently, traditional models are better suited for stable pairs, while advanced models, such as wavelet-augmented LSTM, are more effective for volatile currencies, improving forecasting accuracy for stakeholders.

Figure 11. Model wise Estimated Error Metrices in ascending order of RMSE[30]

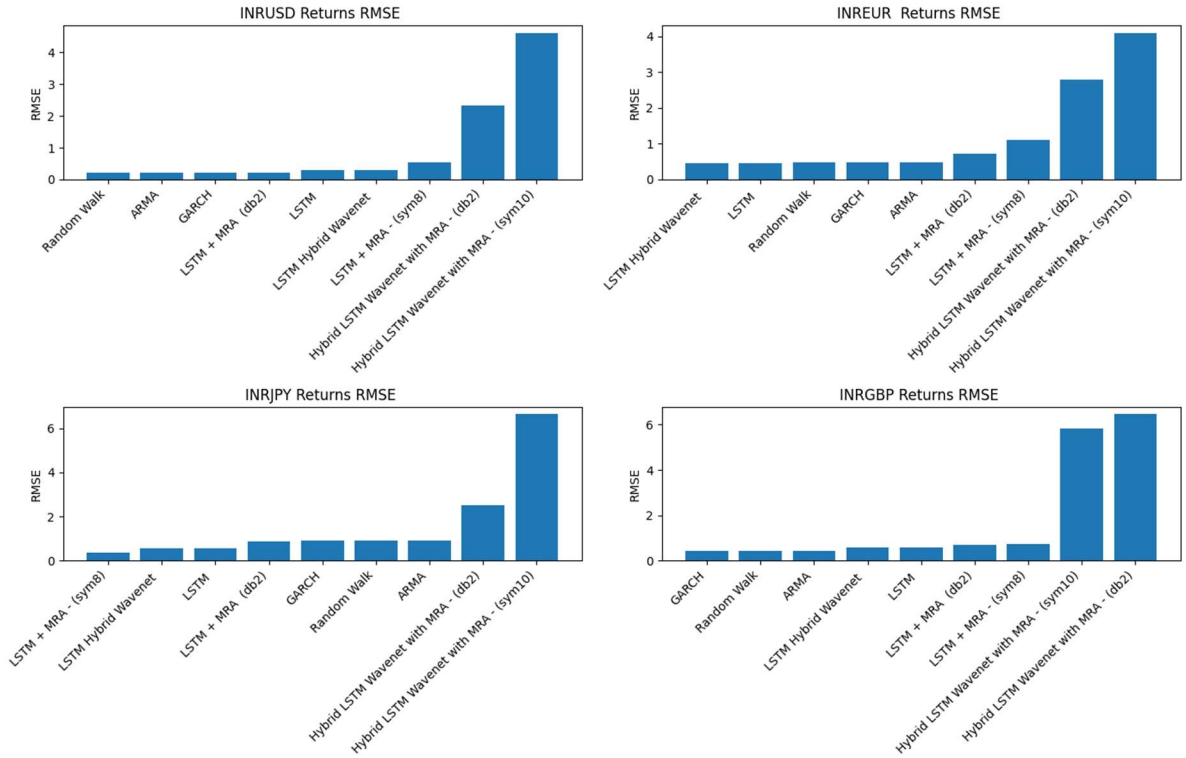

[30] Currency - wise error metrices are presented in Figure 12 of appendix 4

i) Comparing across Machine Learning Approaches (LSTM and Hybrid LSTM models with wavelet activation function

Based on the findings in Figure 11, LSTM models with Multiresolution Analysis (MRA) consistently outperform hybrid LSTM models for INRUSD and INRJPY, highlighting the strength of wavelet-based models in capturing complex, multi-scale patterns in these exchange rate returns. For INREUR and INRGBP, however, hybrid LSTM models with Wavenet activation perform better than other LSTM variants, demonstrating the value of hybrid approaches for these specific currency pairs. Although models using custom activation functions (e.g., the 6th derivative of the sigmoid function) show improvement over simple LSTM models, their performance does not surpass traditional models uniformly across exchange rate return pairs.

The choice of window length and wavelet type significantly affects prediction accuracy. LSTM hybrid Wavenet models with wavelet activation functions showed improved accuracy compared to simple LSTM models, though errors remained higher than traditional ARMA models. This highlights the importance of selecting the right wavelet transforms in the decomposition stage, with Sym8 wavelets yielding the best results for INRUSD, INRJPY, and INRGBP. In contrast, for INREUR, simpler models like the LSTM Hybrid Wavenet without MRA outperformed wavelet-augmented models, indicating that the effectiveness of wavelet-based approaches depends on the specific exchange rate series.

A key insight from this study is the importance of choosing the right mother wavelet. Various wavelets were evaluated (namely, db2, db4, db8, sym2, sym4, sym8, coif1, coif2, haar, bior1.3, bior3.5, and bior6.8), and it was found that certain wavelets capture different aspects of the data more effectively. For example, Sym8 proved particularly robust for predicting INRJPY return series while db2 was more effective in case of INRUSD[31]. The findings emphasize that the choice of wavelet and decomposition technique should be carefully aligned with the characteristics of the time series being predicted. This also highlights the need for further research on parameter tuning and calibration to optimize machine learning models for different financial time series, particularly in the Indian context.

5. Conclusion

This study aimed to determine whether wavelet-based approaches outperform traditional models in forecasting exchange rates by considering different time horizons. By decomposing Indian Rupee (INR) returns relative to the US Dollar (USD), British Pound (GBP), Euro (EUR), and Japanese Yen

31

(JPY) across multiple scales, significant multiscale properties were identified. During financial crises, heightened volatility and contagion effects were observed, particularly for GBP and JPY, as confirmed by DCC-GARCH models and wavelet variance analysis.

Volatility spillovers and long-term persistence, especially in the INR-USD pair, indicate inefficiencies in price discovery, where information transmission is incomplete across currency pairs. Furthermore, the multiscale dynamics show that long memory at broader scales and mean-reversion at shorter scales suggest that markets may exhibit structured but not fully efficient price movements, particularly in the short term.

Forecasting results showed that wavelet-augmented models, particularly hybrid LSTM-Wavenet, excelled in predicting volatile pairs like INRJPY. Traditional models like ARMA performed better for stable pairs like INRUSD and INRGBP, indicating the importance of selecting models based on market complexity and time horizon.

While the findings are promising, future research should explore chaos estimation using prices instead of returns and further optimize wavelet-based models, including tuning translation and dilation parameters. Incorporating high-frequency data and alternative activation functions could also improve prediction accuracy. From a policy perspective, central banks should monitor multiscale dynamics to devise effective strategies during crises, while traders and investors can benefit from scale-specific risk management approaches. Overall, wavelet-based forecasting shows potential in volatile markets, though traditional models remain more effective for stable pairs. Future research should refine these models to enhance forecasting in diverse market conditions.

6. References

Adrian, T., Natalucci, F., & Wu, J. (2024, July 22). Financial stability implications of emerging market currency developments. International Monetary Fund.

Ahmad, W., Rais, S., & Mishra, R. K. (2017). An Analysis of Dynamic Spillover in India's Forex Derivatives Markets. *Theorizing International Trade: An Indian Perspective*, 351-384.

Ahmad, W., Sehgal, S., & Bhanumurthy, N. R. (2013). Eurozone crisis and BRIICKS stock markets: Contagion or market interdependence?. *Economic Modelling*, *33*, 209-225.

Aloui, R., Aïssa, M. S. B., & Nguyen, D. K. (2011). Global financial crisis, extreme interdependences, and contagion effects: The role of economic structure?. *Journal of Banking & Finance*, *35*(1), 130-141.

Andersen, T. G., & Bollerslev, T. (2018). *Volatility*. Edward Elgar Publishing Limited.

Andreou, E., Ghysels, E., & Kourtellos, A. (2013). Should macroeconomic forecasters use daily financial data and how?. *Journal of Business & Economic Statistics*, *31*(2), 240-251.

Armstrong, J. S. (2001). *Selecting forecasting methods* (pp. 365-386). Springer US.

Baillie, R. T. (1996). Long memory processes and fractional integration in econometrics. *Journal of econometrics*, *73*(1), 5-59.

Barkoulas, J. T., Baum, C. F., & Travlos, N. (2000). Long memory in the Greek stock market. *Applied Financial Economics*, *10*(2), 177-184.

Baruník, J., & Kraicová, L. (2014). Estimation of long memory in volatility using wavelets (No. 33/2014). IES Working Paper.

Baruník, J., Kočenda, E., & Vacha, L. (2014). Wavelet-based correlation analysis of the key traded assets. *Wavelet Applications in Economics and Finance*, 157-183.

Bauwens, L., & Sucarrat, G. (2010). General-to-specific modelling of exchange rate volatility: A forecast evaluation. *International Journal of Forecasting*, *26*(4), 885-907.

Bekaert, G. (1995). The Time Variation of Expected Returns and Volatility in Foreign-Exchange Markets. *Journal of Business & Economic Statistics*, *13*(4), 397–408. https://doi.org/10.2307/1392385

Bekaert, G., Harvey, C. R., & Lundblad, C. (2006). Growth volatility and financial liberalization. *Journal of international money and finance*, *25*(3), 370-403.

Bekiros, S., & Marcellino, M. (2013). The multiscale causal dynamics of foreign exchange markets. *Journal of International Money and Finance*, *33*, 282-305.

Bensaïda, A. (2014). Noisy chaos in intraday financial data: Evidence from the American index. *Applied Mathematics and Computation*, *226*, 258-265.

BenSaïda, A. (2015). A practical test for noisy chaotic dynamics. *SoftwareX*, *3*, 1-5.

BenSaïda, A., & Litimi, H. (2013). High level chaos in the exchange and index markets. *Chaos, Solitons & Fractals*, *54*, 90-95.

Bollerslev, T. (1986). Generalized autoregressive conditional heteroskedasticity. *Journal of econometrics*, *31*(3), 307-327.

Breitung, J., & Candelon, B. (2006). Testing for short-and long-run causality: A frequency-domain approach. *Journal of econometrics*, *132*(2), 363-378.

Cajueiro, D. O., & Tabak, B. M. (2004). The Hurst exponent over time: testing the assertion that emerging markets are becoming more efficient. *Physica A: statistical mechanics and its applications*, *336*(3-4), 521-537.

Calvo, S. G., & Reinhart, C. (1996). Capital flows to Latin America: is there evidence of contagion effects?. *Available at SSRN 636120*.

Chan, K. S., & Tong, H. (2013). *Chaos: a statistical perspective*. Springer Science & Business Media.

Chortareas, G., Jiang, Y., & Nankervis, J. C. (2011). Forecasting exchange rate volatility using high-frequency data: Is the euro different?. *International Journal of Forecasting*, *27*(4), 1089-1107.

Conlon, T., & Cotter, J. (2012). An empirical analysis of dynamic multiscale hedging using wavelet decomposition. *Journal of Futures Markets*, *32*(3), 272-299.

Connor, J., & Rossiter, R. (2005). Wavelet transforms and commodity prices. *Studies in Nonlinear Dynamics & Econometrics*, *9*(1).

Corsi, F. (2009). A simple approximate long-memory model of realized volatility. *Journal of Financial Econometrics*, *7*(2), 174-196.

Crowley, P. M. (2007). A guide to wavelets for economists. *Journal of Economic Surveys*, *21*(2), 207-267.

Crowley, P. M., & Hallett, A. H. (2021). The evolution of US and UK real GDP components in the time-frequency domain: a continuous wavelet analysis. *Journal of Business Cycle Research*, *17*(3), 233-261.

Crowley, P. M., & Hudgins, D. (2024). The impact of US productivity growth on unemployment in the time–frequency domain: is AI causing a change in the relationship?. *Empirical Economics*, *66*(5), 2169-2190.

Datta, R. P., & Bhattacharyya, R. (2018). Predictability of Indian Exchange Rates. *The Journal of Prediction Markets*, *12*(3), 1-22.

Daubechies, I. (1992). Ten lectures on wavelets. Society for industrial and applied mathematics.

De Grauwe, P., & Grimaldi, M. (2006). Exchange rate puzzles: a tale of switching attractors. *European Economic Review*, *50*(1), 1-33.

Del Negro, M., & Schorfheide, F. (2013). DSGE model-based forecasting. In *Handbook of economic forecasting* (Vol. 2, pp. 57-140). Elsevier.

Diebold, F. X., & Yilmaz, K. (2009). Measuring financial asset return and volatility spillovers, with application to global equity markets. *The Economic Journal*, *119*(534), 158-171.

Dornbusch, R., Park, Y. C., & Claessens, S. (2000). Contagion: Understanding how it spreads. *The World Bank Research Observer*, *15*(2), 177-197.

Dua, P., & Ranjan, R. (2011). *Modelling and forecasting the Indian RE/US dollar exchange rate* (Vol. 197). CDE.

Dunis, C., Likothanassis, S., Karathanasopoulos, A., Sermpinis, G., & Theofilatos, K. (Eds.). (2014). *Computational intelligence techniques for trading and investment*. London: Routledge.

Edwards, S., & Susmel, R. (2001). Volatility dependence and contagion in emerging equity markets. *Journal of Development Economics*, *66*(2), 505-532.

Eichengreen, B., Park, D., & Shin, K. (2012). When fast-growing economies slow down: International evidence and implications for China. *Asian Economic Papers*, *11*(1), 42-87.

Eichengreen, B., Rose, A. K., & Wyplosz, C. (1996). Contagious currency crises.

Engle, R. (2002). Dynamic conditional correlation: A simple class of multivariate generalized autoregressive conditional heteroskedasticity models. *Journal of business & economic statistics*, *20*(3), 339-350.

Engle, R. F. (1982). Autoregressive Conditional Heteroscedasticity with Estimates of the Variance of United Kingdom Inflation. *Econometrica, 50*(4), 987-1007. https://doi.org/10.2307/1912773

Fair, R. C. (1986). Interest rate and exchange rate determination.

Fama, E. F. (1970). Efficient capital markets: A review of theory and empirical work. The Journal of Finance, 25(2), 383-417.

Fernandez, V. (2008). Multi-period hedge ratios for a multi-asset portfolio when accounting for returns co-movement. *Journal of Futures Markets: Futures, Options, and Other Derivative Products*, *28*(2), 182-207.

Fernandez, V. P. (2005). The international CAPM and a wavelet-based decomposition of value at risk. *Studies in Nonlinear Dynamics & Econometrics*, *9*(4).

Fernández-Macho, J. (2012). Wavelet multiple correlation and cross-correlation: A multiscale analysis of Eurozone stock markets. *Physica A: Statistical Mechanics and its Applications*, *391*(4), 1097-1104.

Forbes, K. J., & Chinn, M. D. (2004). A decomposition of global linkages in financial markets over time. Review of economics and statistics, 86(3), 705-722.

Forbes, K. J., & Rigobon, R. (2002). No contagion, only interdependence: measuring stock market comovements. The Journal of Finance, 57(5), 2223-2261.

Frankel, J. A. (1979). On the mark: A theory of floating exchange rates based on real interest differentials. *The American economic review*, *69*(4), 610-622.

Friedman, M. (1957). The permanent income hypothesis. In *A theory of the consumption function* (pp. 20-37). Princeton University Press.

Froot, K. A., & Rogoff, K. (1995). Perspectives on PPP and long-run real exchange rates. *Handbook of international economics*, *3*, 1647-1688.

Gallegati, M., & Gallegati, M. (2007). Wavelet variance analysis of output in G-7 countries. *Studies in Nonlinear Dynamics & Econometrics*, *11*(3).

Gardner Jr, E. S. (1985). Exponential smoothing: The state of the art. *Journal of forecasting*, *4*(1), 1-28.

Gençay, R., Selçuk, F., & Whitcher, B. (2001a). Differentiating intraday seasonalities through wavelet multi-scaling. *Physica A: Statistical Mechanics and its Applications*, *289*(3-4), 543-556.

Gençay, R., Selçuk, F., & Whitcher, B. J. (2001). *An introduction to wavelets and other filtering methods in finance and economics*. Elsevier.

Gleick, J. (2008). *Chaos: Making a new science*. Penguin.

Glick, R., & Rose, A. K. (1999). Contagion and trade: why are currency crises regional?. *Journal of international Money and Finance*, *18*(4), 603-617.

Glosten, L. R., Jagannathan, R., & Runkle, D. E. (1993). On the relation between the expected value and the volatility of the nominal excess return on stocks. *The journal of finance*, *48*(5), 1779-1801.

Gong, J., Wang, G. J., Zhou, Y., Zhu, Y., Xie, C., & Foglia, M. (2023). Spreading of cross-market volatility information: Evidence from multiplex network analysis of volatility spillovers. *Journal of International Financial Markets, Institutions and Money*, *83*, 101733.

Gradojevic, N., Erdemlioglu, D., & Gençay, R. (2020). A new wavelet-based ultra-high-frequency analysis of triangular currency arbitrage. *Economic Modelling*, *85*, 57-73.

Granero, M. S., Segovia, J. T., & Pérez, J. G. (2008). Some comments on Hurst exponent and the long memory processes on capital markets. *Physica A: Statistical Mechanics and its applications*, *387*(22), 5543-5551.

Granger, C. W., & Joyeux, R. (1980). An introduction to long-memory time series models and fractional differencing. *Journal of time series analysis*, *1*(1), 15-29.

Grau-Carles, P. (2005). Tests of long memory: A bootstrap approach. Computational Economics, 25(1-2), 103-113.

Grossmann, A., & Morlet, J. (1984). Decomposition of Hardy functions into square integrable wavelets of constant shape. *SIAM journal on mathematical analysis*, 15(4), 723-736.

Hanke, J. E., & Wichern, D. W. (2013). *Business Forecasting: Pearson New International Edition*. Pearson Higher Ed.

He, X., Gokmenoglu, K. K., Kirikkaleli, D., & Rizvi, S. K. A. (2023). Co-movement of foreign exchange rate returns and stock market returns in an emerging market: Evidence from the wavelet coherence approach. *International Journal of Finance & Economics*, *28*(2), 1994-2005.

Hernández, L. F., & Valdés, R. O. (2001). What drives contagion: trade, neighborhood, or financial links?. *International Review of Financial Analysis*, *10*(3), 203-218.

Hommes, C. H. (2006). Heterogeneous agent models in economics and finance. *Handbook of computational economics*, *2*, 1109-1186.

Hong, Y., & Lee, T. H. (2003). Inference on predictability of foreign exchange rates via generalized spectrum and nonlinear time series models. *Review of Economics and Statistics*, *85*(4), 1048-1062.

Hurst, H. E. (1951). Long-term storage capacity of reservoirs. *Transactions of the American society of civil engineers*, *116*(1), 770-799.

In, F., & Kim, S. (2013). *An introduction to wavelet theory in finance: a wavelet multiscale approach*. World scientific.

Jensen, M. J. (1999). Using wavelets to obtain a consistent ordinary least squares estimator of the long-memory parameter. *Journal of forecasting*, *18*(1), 17-32.

Jensen, M. J., & Whitcher, B. (2014). Measuring the impact intradaily events have on the persistent nature of volatility. In *Wavelet Applications in Economics and Finance* (pp. 103-129). Cham: Springer International Publishing.

Kaminsky, G. L., & Reinhart, C. M. (2000). On crises, contagion, and confusion. *Journal of international Economics*, *51*(1), 145-168.

Kantz, H., & Schreiber, T. (2004). *Nonlinear time series analysis* (Vol. 7). Cambridge university press.

Karolyi, G. A. (2004). Does international financial contagion really exist?. *Journal of Applied Corporate Finance*, *16*(2-3), 136-146.

Kılıç, D. K., & Uğur, Ö. (2023). Hybrid wavelet-neural network models for time series. *Applied Soft Computing*, *144*, 110469.

Killick, R., Fearnhead, P., & Eckley, I. A. (2012). Optimal detection of changepoints with a linear computational cost. *Journal of the American Statistical Association*, *107*(500), 1590-1598.

Kim, S., & In, F. (2005). The relationship between stock returns and inflation: new evidence from wavelet analysis. *Journal of empirical finance*, *12*(3), 435-444.

King, M. A., & Wadhwani, S. (1990). Transmission of volatility between stock markets. *The review of financial studies*, *3*(1), 5-33.

Kodres, L. E., & Pritsker, M. (2002). A rational expectations model of financial contagion. *The journal of finance*, *57*(2), 769-799.

Kuşkaya, S., Toğuç, N., & Bilgili, F. (2022). Wavelet coherence analysis and exchange rate movements. *Quality & Quantity*, *56*(6), 4675-4692.

Lahmiri, S. (2017). Investigating existence of chaos in short and long term dynamics of Moroccan exchange rates. *Physica A: Statistical Mechanics and its Applications*, *465*, 655-661.

Lahmiri, S. (2017). On fractality and chaos in Moroccan family business stock returns and volatility. *Physica A: Statistical Mechanics and its Applications*, *473*, 29-39.

Lindé, J., Smets, F., & Wouters, R. (2016). Challenges for central banks' macro models. In *Handbook of macroeconomics* (Vol. 2, pp. 2185-2262). Elsevier.

Lütkepohl, H. (2005). *New introduction to multiple time series analysis*. Springer Science & Business Media.

Makridakis, S., Hogarth, R. M., & Gaba, A. (2010). Why forecasts fail. What to do instead. *MIT Sloan Management Review*, *51*(2), 83.

Mallat, S. G. (1989). A theory for multiresolution signal decomposition: the wavelet representation. IEEE transactions on pattern analysis and machine intelligence, 11(7), 674-693.

Mandelbrot, B. B., & Wallis, J. R. (1969). Robustness of the rescaled range R/S in the measurement of noncyclic long run statistical dependence. *Water resources research*, *5*(5), 967-988.

Martens, M. (2001). Forecasting daily exchange rate volatility using intraday returns. *Journal of International Money and Finance*, *20*(1), 1-23.

McGuire, P. (2022). Triennial Central Bank Survey of Foreign Exchange and Over-the-Counter (OTC) Derivatives Markets in 2022. *BIS (Bank of International Settlements), October*, *27*, 2022.

Meese, R. A., & Rogoff, K. (1983). Empirical exchange rate models of the seventies: Do they fit out of sample?. *Journal of international economics*, *14*(1-2), 3-24.

Mehra, Y. P., & Sawhney, B. (2010). Inflation measure, Taylor rules, and the Greenspan-Bernanke years. *FRB Richmond Economic Quarterly*, *96*(2), 123-151.

Meng, X., & Huang, C. H. (2019). The time-frequency co-movement of Asian effective exchange rates: A wavelet approach with daily data. *The North American Journal of Economics and Finance*, *48*, 131-148.

Mensi, W., Tiwari, A. K., & Al-Yahyaee, K. H. (2019). An analysis of the weak form efficiency, multifractality and long memory of global, regional and European stock markets. *The Quarterly Review of Economics and Finance*, *72*, 168-177.

Meyer, Y. (1992). Wavelets and Operators: Volume 1 (No. 37). Cambridge university press.

Mishra, R. K., Sehgal, S., & Bhanumurthy, N. R. (2011). A search for long-range dependence and chaotic structure in Indian stock market. *Review of Financial Economics*, *20*(2), 96-104.

Mitra, S., & Mitra, A. (2006). Modeling exchange rates using wavelet decomposed genetic neural networks. *Statistical Methodology*, *3*(2), 103-124.

Müller, U. A., Dacorogna, M. M., Davé, R. D., Olsen, R. B., Pictet, O. V., & Von Weizsäcker, J. E. (1997). Volatilities of different time resolutions—analyzing the dynamics of market components. *Journal of Empirical Finance*, *4*(2-3), 213-239.

Muth, J. F. (1961). Rational expectations and the theory of price movements. *Econometrica: journal of the Econometric Society*, 315-335.

Nachane, D. M. (2018). Time-varying spectral analysis: Theory and applications. *Indian Economic Review*, *53*, 3-27.

Nelson, D. B. (1991). Conditional heteroskedasticity in asset returns: A new approach. *Econometrica: Journal of the econometric society*, 347-370.

Nychka, D., Ellner, S., Gallant, A. R., & McCaffrey, D. (1992). Finding chaos in noisy systems. *Journal of the Royal Statistical Society: Series B (Methodological)*, *54*(2), 399-426.

Olayeni, O. R. (2016). Causality in continuous wavelet transform without spectral matrix factorization: theory and application. *Computational Economics*, *47*(3), 321-340.

Park, J. Y., & Whang, Y. J. (2012). Random walk or chaos: A formal test on the Lyapunov exponent. *Journal of Econometrics*, *169*(1), 61-74.

Percival, D. B., & Walden, A. T. (2000). *Wavelet methods for time series analysis* (Vol. 4). Cambridge university press.

Pir, M. Y. (2022). Applications of Wavelet Neural Networks in Financial Time Series.

Priewe, J. (2017). Review of exchange-rate theories in four leading economics textbooks. *European Journal of Economics and Economic Policies*, *14*(1), 32-47.

Ramsey, J. B. (2002). Wavelets in economics and finance: Past and future. *Studies in Nonlinear Dynamics & Econometrics*, *6*(3).

Ramsey, J. B., & Lampart, C. (1998). Decomposition of economic relationships by timescale using wavelets. *Macroeconomic dynamics*, *2*(1), 49-71.

Ramsey, J. B., & Zhang, Z. (1996). The application of wave form dictionaries to stock market index data. In *Predictability of complex dynamical systems* (pp. 189-205). Berlin, Heidelberg: Springer Berlin Heidelberg.

Ramsey, J. B., & Zhang, Z. (1997). The analysis of foreign exchange data using waveform dictionaries. *Journal of Empirical Finance*, *4*(4), 341-372.

Rigobon, R. (2003). On the measurement of the international propagation of shocks: is the transmission stable?. Journal of International Economics, 61(2), 261-283.

Rogoff, K. S., & Stavrakeva, V. (2008). *The continuing puzzle of short horizon exchange rate forecasting* (No. w14071). National Bureau of Economic Research.

Ronderos. N. (2016). Spectral Granger Causality Test* - EViews.com. (n.d.). Retrieved from https://forums.eviews.com/viewtopic.php?t=15114

Roventini, A., & Fagiolo, G. (2017). Macroeconomic policy in DSGE: methodological pitfalls, patches or new clothes?. In *Theory and Method of Evolutionary Political Economy* (pp. 143-165). Routledge.

Rua, A. 2013. "Worldwide Synchronization since the Nineteenth Century: A Wavelet Based View." *Applied Economics Letters* 20 (8): 773–776.

Schleicher, C. (2002). *An introduction to wavelets for economists* (No. 2002-3). Bank of Canada.

Selçuk, F., & Gençay, R. (2006). Intraday dynamics of stock market returns and volatility. *Physica A: Statistical Mechanics and its Applications*, *367*, 375-387.

Sen, C., & Chakrabarti, G. (2014). The efficacy of intervention in a chaotic foreign exchange market: an empirical study in INR-USD exchange rate series. *Decision*, *41*, 399-410.

Shahrier, N. A. (2022). Contagion effects in ASEAN-5 exchange rates during the Covid-19 pandemic. *The North American Journal of Economics and Finance*, *62*, 101707.

Sims, C. A. (1980). Macroeconomics and reality. *Econometrica: journal of the Econometric Society*, 1-48.

Singhal, D., & Swarup, K. S. (2011). Electricity price forecasting using artificial neural networks. *International Journal of Electrical Power & Energy Systems*, *33*(3), 550-555.

Tan, Z., Zhang, J., Wang, J., & Xu, J. (2010). Day-ahead electricity price forecasting using wavelet transform combined with ARIMA and GARCH models. *Applied energy*, *87*(11), 3606-3610

Teyssière, G., & Abry, P. (2007). Wavelet analysis of nonlinear long-range dependent processes. Applications to financial time series. *Long memory in economics*, 173-238.

Venkatesh, H., & Hiremath, G. S. (2020). Currency mismatches in emerging market economies: Is winter coming?. *Bulletin of Monetary Economics and Banking*, *23*(1), 25-54.

Vo, L. H., & Vo, D. H. (2020). Modelling Australian dollar volatility at multiple horizons with high-frequency data. *Risks*, *8*(3), 89.

Vogl, M. (2022). Controversy in financial chaos research and nonlinear dynamics: a short literature review. *Chaos, Solitons & Fractals*, *162*, 112444.

Welch, P. (1967). The use of fast Fourier transform for the estimation of power spectra: a method based on time averaging over short, modified periodograms. *IEEE Transactions on audio and electroacoustics*, *15*(2), 70-73.

Wen, X. B., Zhang, H., & Wang, F. Y. (2009). A wavelet neural network for SAR image segmentation. *Sensors*, *9*(9), 7509-7515.

Weron, R. (2002). Estimating long-range dependence: finite sample properties and confidence intervals. *Physica A: Statistical Mechanics and its Applications*, *312*(1-2), 285-299.

Westerhoff, F. H. (2009). Exchange rate dynamics: A nonlinear survey. In *Handbook of research on complexity*. Edward Elgar Publishing.

Yazgan, M. E., & Özkan, H. (2015). Detecting structural changes using wavelets. *Finance Research Letters*, *12*, 23-37.

Yousefi, S., Weinreich, I., & Reinarz, D. (2005). Wavelet-based prediction of oil prices. *Chaos, Solitons & Fractals*, *25*(2), 265-275.

Yu, X. (2013). Measurement error and policy evaluation in the frequency domain. *Journal of Macroeconomics*, *38*, 307-329.

Yueh, L. (2023). The Great Crashes: Lessons from Global Meltdowns and How to Prevent Them. London: Penguin Business.

Yueh, L. (2023). *The Great Crashes: Lessons from Global Meltdowns and How to Prevent Them*. Penguin UK.

Živkov, D., Kuzman, B., & Andrejević-Panić, A. (2021). Nonlinear bidirectional multiscale volatility transmission effect between stocks and exchange rate markets in the selected African countries. *Economic research-Ekonomska istraživanja*, *34*(1), 1623-1650.

Appendix 1 - Methodology

I. Wavelets and Multiresolution Analysis

i) Wavelets

Wavelets are mathematical functions used to decompose data into various frequency components, allowing for analysis at a resolution appropriate to each scale. They grow and decay in a limited time (Percival and Walden, 2000). Mathematically, in general, form a wavelet for a time series x(t) on $L^2\mathbb{R}$ is represented as:

$$X_{a,b} = \int_{-\infty}^{\infty} x(t)\, \psi_{a,b}\, t(dt) \qquad (i)$$

Where x(t) is the process, , $\psi_{a,b}$ is the arbitrary mother wavelet transform, a is the scaling (i.e., stretching or compressing a signal), and b is the translation parameter. The basis of a wavelet transform is shifted and scaled versions of the time-localized, *compactly supported* (i.e., non-zero over finite time span) mother wavelet, which is given as:

$$\psi_{a,b}(t) = \psi_{a,b}(t) = \frac{1}{\sqrt{s}}\psi\left(\frac{t-b}{s}\right) \qquad (ii)$$

where s≠ 0 and b are real constants, *s* is the scaling or dilation parameter (used to determine window widths), where scale = 1/ frequency, and *b* is the translation or shifting parameter (which controls the window's location). The scaling function decomposes a given time signal into approximation and detail components. The admissibility condition is a fundamental requirement for wavelets used, especially in Continuous wavelet transform (CWT) and scalogram analysis. In functional form, it is represented as $\wedge(0) = 0, where\ \wedge(.)$ is the Fourier transform of the mother wavelet or $\sum_{t=-\infty}^{\infty} \psi_{a,b}(t) = 0$ in the time domain[32].

II. Long memory Estimation

To perform the R/S analysis on the exchange rate returns series, the data is partitioned into various segments with different lengths. Subsequently, the range of each segment is computed by finding the difference between the maximum and minimum values within that segment. Next, the rescaled range is obtained by dividing the calculated range by the standard deviation of the entire time series. Finally, the Hurst exponent is estimated by determining the slope of the plot generated by taking the logarithm of the rescaled range (log(R/S)) against the logarithm of the segment length (log(segment length)). The Hurst exponent is calculated as follows :

First, for the exchange rate returns series x_i of length T , with the mean $\bar{x}$ and standard deviation s_t , the data is rescaled to having zero mean by taking deviation from each observation. By adding each rescaled sample from second observation onwards in turn to first rescaled observation, a cumulative series is created.

$$Y_j = \left((x_i - \bar{x}) + \left(x_j - \bar{x}\right)\right) \qquad (iii)$$

and adjusted range R_n is calculated as

$$R_n = max \sum_{i=1}^{t}((x_i - \bar{x})_i)_t - min \sum_{i=1}^{t}((x_i - \bar{x})_i)_t \ \ , t = 1 \ldots . n \qquad (iv)$$

Which leads to the formula,

[32] For proof on the derivation of wavelet coefficients, refer to Appendix 12.A5, (Woodward et al. 2012 pp. 475-476)

$$\frac{R_n}{s_n} = C * n^H \quad (v)$$

Where, R_n is the adjusted range, s_n is the standard deviation, n is the window size, and H is the Hurst exponent. $\frac{R_n}{s_n}$ is known as the rescaled range.

Further, Anis-Loyd corrected Hurst exponent (H*) is estimated, which corrects the bias in H to estimate the true long-term scaling behavior better when dealing with real (finite) time series data. In equation form, it is given as:

$$E\left(\frac{R}{S}\right)_n = \begin{cases} \dfrac{(n-0.5)\tau\left(\frac{n-1}{2}\right)}{n\sqrt{\pi}\tau\left(\frac{n}{2}\right)} \sum_{i=1}^{n-1}\sqrt{\dfrac{n-i}{i}} & for\ n \leq 340, \\ \dfrac{(n-0.5)}{n\sqrt{\frac{n\pi}{2}}} \sum_{i=1}^{n-1}\sqrt{\dfrac{n-i}{i}} & for\ n \leq 340, \end{cases}$$

$$\frac{R}{S} - AL = \left(\frac{R}{S}\right)_n - E\left(\frac{R}{S}\right)_n + \sqrt{\frac{n\pi}{2}} \quad (vi)$$

Where slope of $\left(\frac{R}{S}\right)_n$ vs Log-Log plot is the classic Hurst exponent and the slope of R/S-AL vs Log-Log plot is the AL corrected Hurst exponent. A Hurst exponent of 0.5 implies a random process, the value in the range $0.5 < H \leq 1$ confirms persistence and long memory in the series, and $0 \leq H < 0.5$ signifies an anti - persistent mean reversion behavior.

III. Chaos Identification

We use the Maximal Lyapunov Exponent (MLE) to test for chaos in returns, estimating the MLE for each MODWT component following Bensaïda et al. (2013, 2014, 2015), Litimi (2013), and Lahmiri (2017). This approach tests for chaotic behavior at various MODWT scales. A positive Lyapunov exponent indicates chaos.

Unlike the stationary wavelet transform (SWT), MODWT does not require a dyadic length series and skips down-sampling, providing more efficient insights. Our goal is to identify chaos at different scales in exchange rates decomposed using MODWT.

To estimate the Lyapunov exponent and test for chaos, we consider a noisy, chaotic system of time series $\{y_t\}_{t=1}^{T}$ which can be expressed as:

$$y_t = f(y_{t-\tau}, y_{t-2\tau}, \ldots\ldots, y_{t-m\tau}) + \varepsilon_t$$

where τ is the time delay, m is the embedding dimension, ε is the noise term, f is an unknown function to approximate chaotic map, and t is the time. For a noise-free system, $Var(\varepsilon_t) = 0$, the Lyapunov exponent (λ) is : $$\lambda = \lim_{M\to\infty} \frac{1}{2M} \log(v_1) \quad (vii)$$

Where v_1 is the maximum eigenvalue of matrix ${T'}_M T_M$ and $T_M = \prod_{t=1}^{M-1} J_{M-1}$ Here, J is the Jacobian matrix of chaotic map f. The unknown chaotic map f is approximated using a multilayer feed-forward neural network (FFNN) trained with a gradient descent algorithm (BenSaïda and Litimi (2013); BenSaïda (2014; Nyschka et al. (1997)), given by :

$$y_t \approx \alpha_0 + \sum_{j=1}^{q} \alpha_j A\left(\beta_{0,j} + \sum_{i=1}^{m} \beta_{i,j}\, y_{t-i\tau}\right) + \varepsilon_t \quad (viii)$$

where q us the number of hidden layers, α_0 is the bias in network, and A is an activation function to process the data. The test statistic for chaos is $\widehat{W} = \sqrt{M} * \hat{\lambda}_M$ where $\widehat{W} \sim N(0, \widehat{\sum})$. The null hypothesis $H_0: \lambda \geq 0$ tests for chaotic dynamics in the time series. The figure below presents the architecture of FNFNN:

Figure.4. Feed Forward Neural Network Architecture

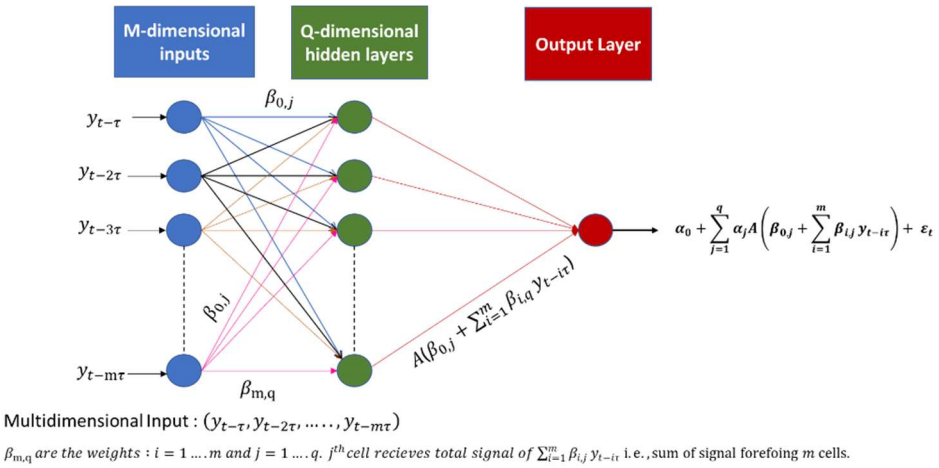

Appendix 2

2.1. On the choice of wavelet transform

Broadly, there are two basic wavelet transforms, i.e., the continuous wavelet transform (CWT) and the discrete wavelet transform (DWT). The CWT is redundant, and it generates a large number of coefficients. On the contrary, DWT has two forms. One is decimated, i.e., Maximal Overlap Discrete Wavelet Transform (MODWT), and generates more coefficients; the other is decimated (Multi-Resolution Analysis), which generates fewer coefficients. Further, CWT and non-decimated DWT are shift-invariant, while the decimated DWT is not shift-invariant as it down samples. From an application perspective, DWT is preferred to obtain the sparsest possible representation of time series for compression and denoising. If the objective requires energy conservation, i.e., orthogonal transform, then DWT with orthogonal wavelet filter should be the choice.

Further, if the application requires perfect reconstruction of the decomposed time series, then non-decimated DWT, i.e., MODWT, should be the choice. The CWT becomes a clear choice in applications where the primary goal is to get a detailed time-frequency (scale) analysis or precise localization of transients in time series, such as discontinuity detection and frequency break. The MODWT can handle any sample size regardless of whether it is dyadic. It remains invariant to translation (i.e., not sensitive to the choice of the starting point of the underlying process) and is a more asymptotically efficient estimator of wavelet variance than DWT (Percival and Mofjeid, 1997). Overall, the choice of wavelet depends on the objective-specific requirements.

Given the objective of this study, for examining the multiscale characteristics, we consider an orthogonal wavelet basis, i.e., Daubechies (db) family with the vanishing moment of 4, which provides a better localization of high-frequency components in the data. It further allows for perfect space reconstruction by keeping the energy of the time series intact. For the long memory and fractality properties, db can capture the slow transitions in data. A wavelet basis with higher vanishing moments is better suited to account for the volatility spillovers along with other scale-wide properties, which the

db4 provides. A wavelet with higher vanishing moments is also more regular and offers more filter length. The Daubechies wavelet with 4 vanishing moments is depicted in figure 3 below:

Fig.3 Daubechies with 4 vanishing moments

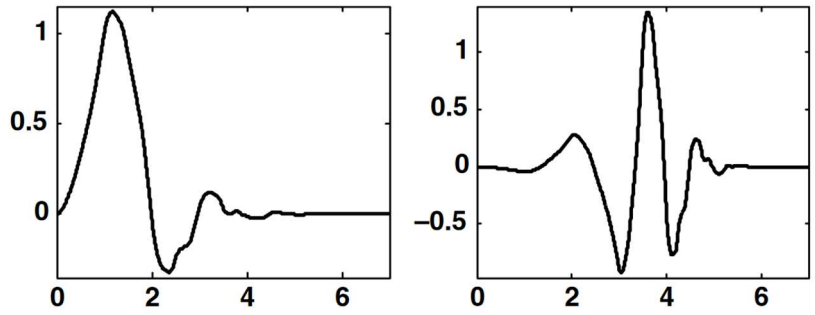

Scaling function Wavelet function

LSTM Configuration and Architecture used for forecasting

Model – wise configuration of LSTM and Hybrid LSTM for scale wide estimation

LSTM model	Hybrid LSTM-WaveNet with MRA		
	Approximation coefficients		Detail Coefficients
Training:Testing:Validation			
Loss Function	RMSE and MAE	RMSE and MAE	RMSE and MAE
Optimiser	Adam	Adam	Adam
Time Steps	10	10	10
Batch Size	1024	1024	1024
Epochs	100	100	100
Layer Parameters			
Nodes in LSTM Layer	16	16	128
Nodes in Dense Layer	128	128	128
Kernel Initializer	default	default	default
Batch Normalization	default	default	default
Activation Function in LSTM Layer	-	6th Derivative of Polynomial Power of Sigmoid	6th Derivative of Polynomial Power of Sigmoid
Activation Function in Dense Layer	ReLU	ReLU	-
Activation Function between Convolutional Layers	ReLU	ReLU	-
Number of Experiments	1000	1000	1000

LSTM Architecture

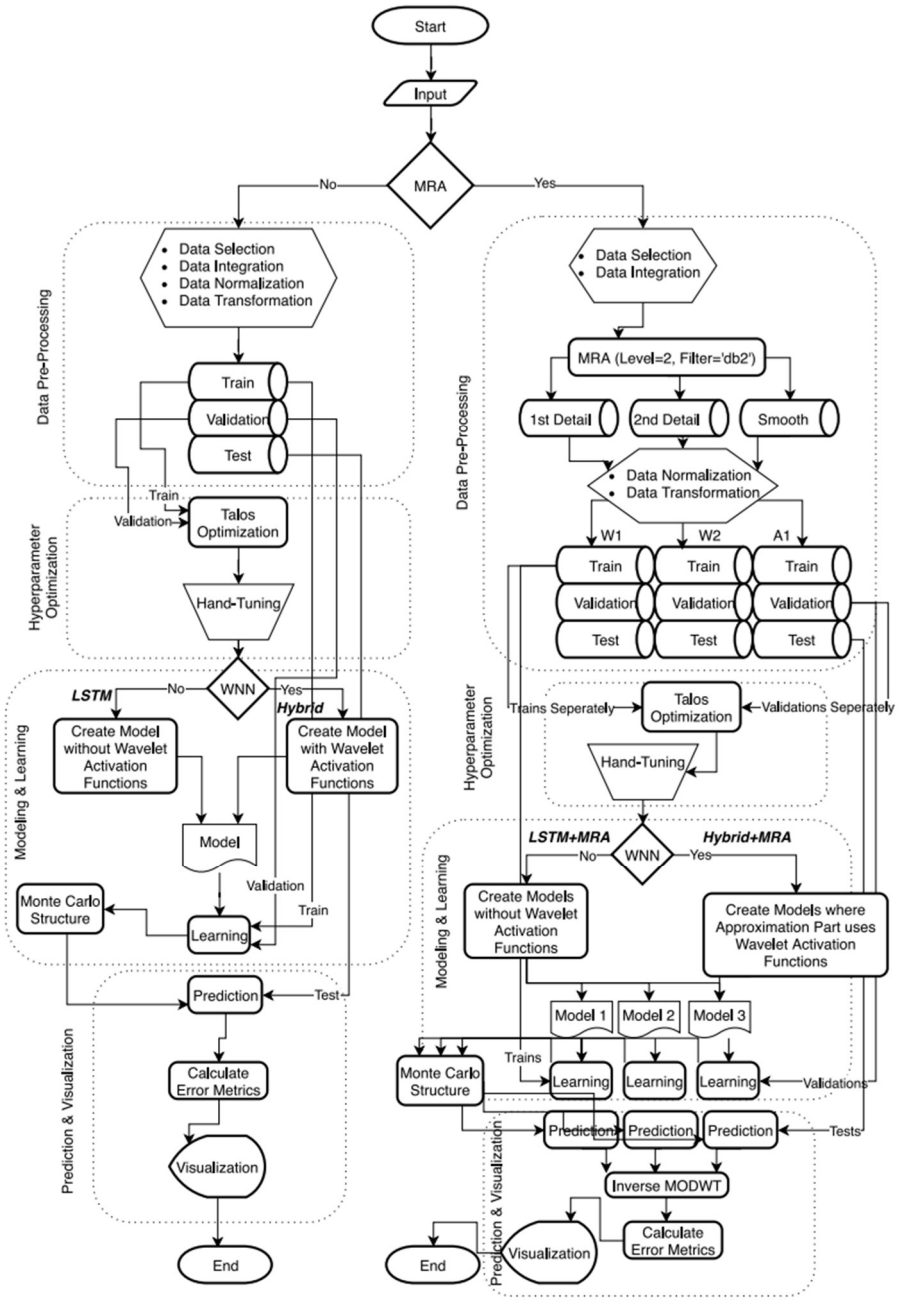

Source: (Kılıç and Uğur,2023)

Configuration for comparing traditional models with LSTM and wavelet based hybrid versions :

Model	Batch size, Epochs	Wavelet Used
LSTM	16, 100	N/A
LSTM + MRA	32*, 100	db2, sym8, sym 10
Hybrid LSTM Wavenet	64, 100	NA
Hybrid LSTM Wavenet with MRA	32, 100	Db2, sym8, sym 10

Note :* For EURINR returns pair, the optimal batch size with lowest error was 16.

Mother wavelets considered in Hybrid – Wavenet LSTM forecasting

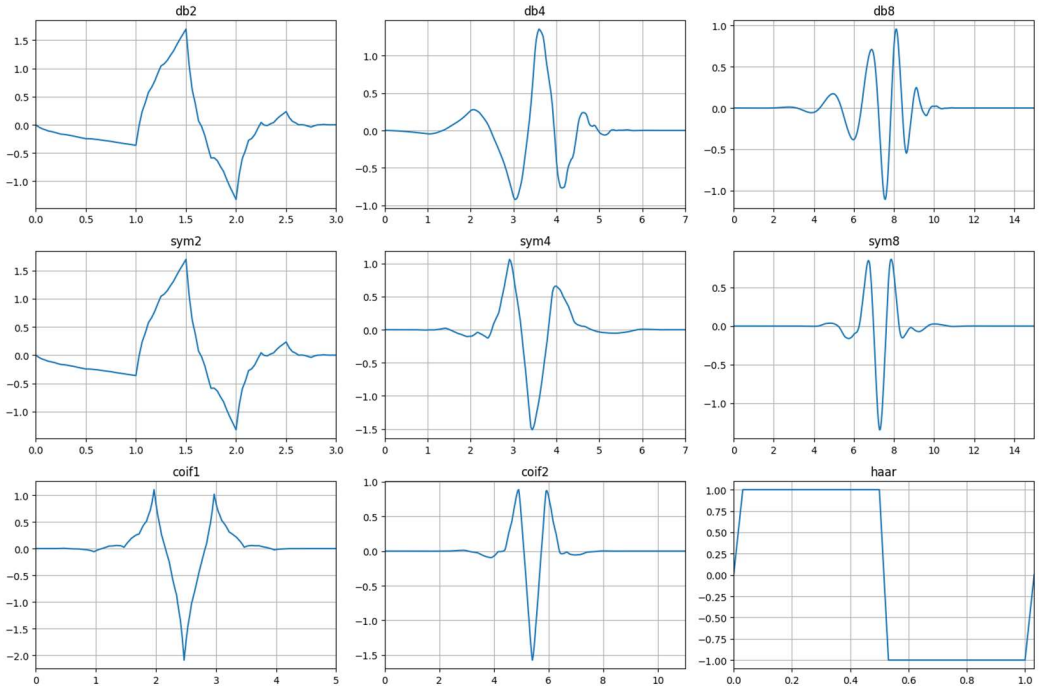

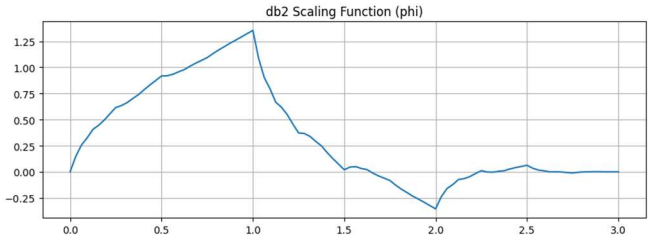
db2 Scaling Function (phi)

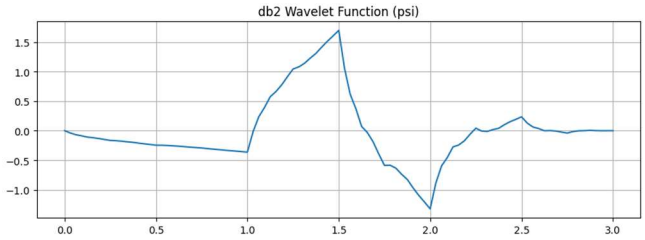
db2 Wavelet Function (psi)

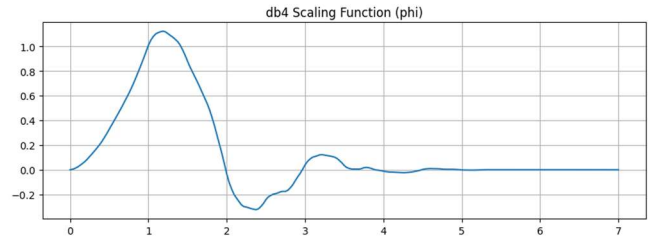
db4 Scaling Function (phi)

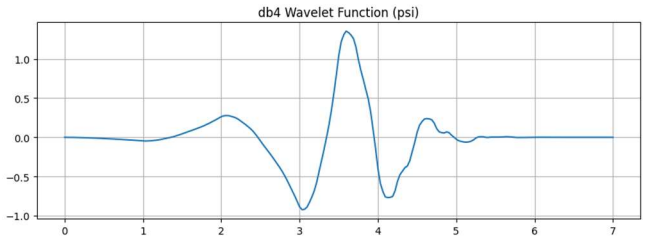
db4 Wavelet Function (psi)

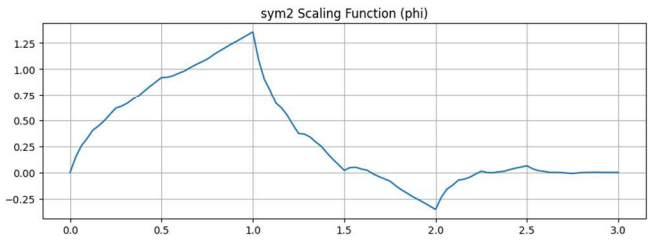
sym2 Scaling Function (phi)

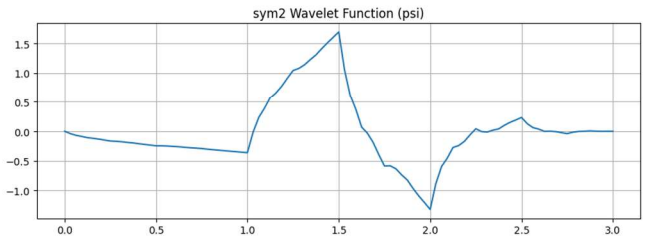
sym2 Wavelet Function (psi)

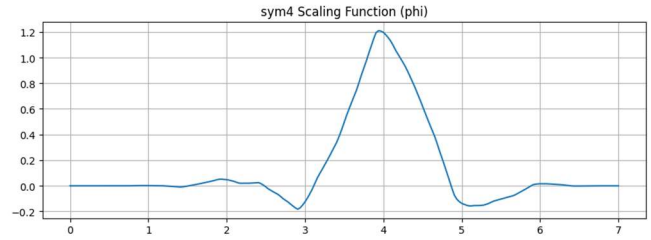
sym4 Scaling Function (phi)

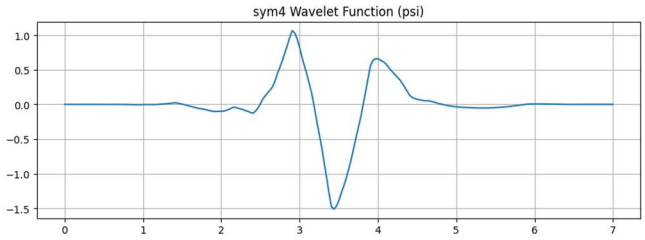
sym4 Wavelet Function (psi)

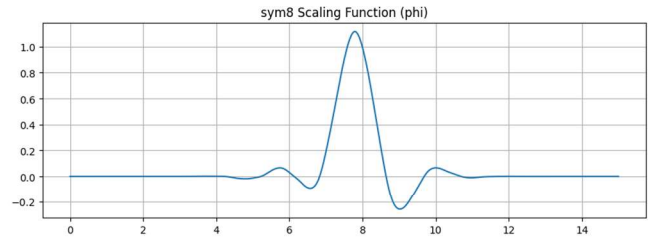
sym8 Scaling Function (phi)

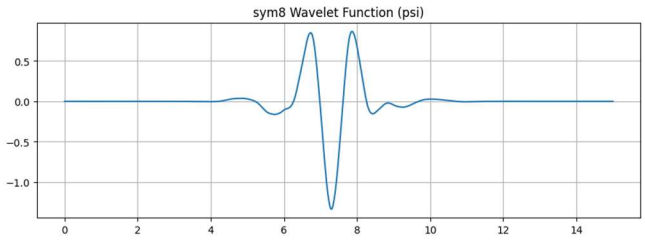
sym8 Wavelet Function (psi)

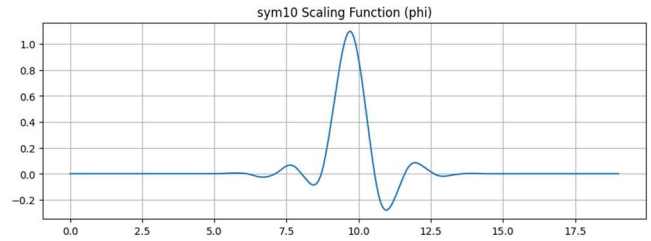
sym10 Scaling Function (phi)

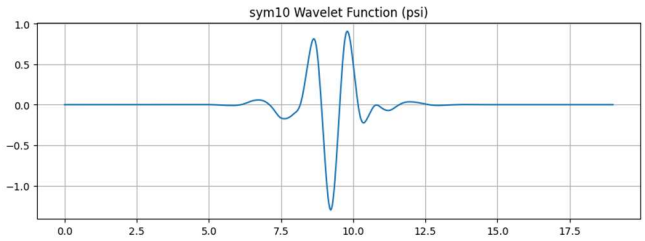
sym10 Wavelet Function (psi)

Appendix 3

Figure 2. a. Log of Bilateral Exchange Rates and their Returns

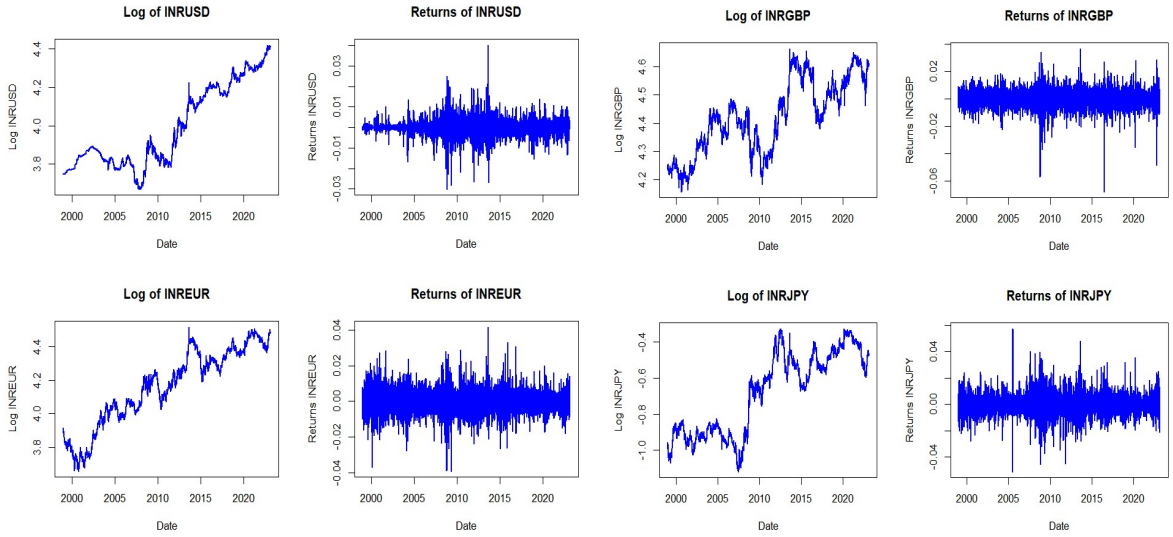

Figure 2.b. Distribution of Returns

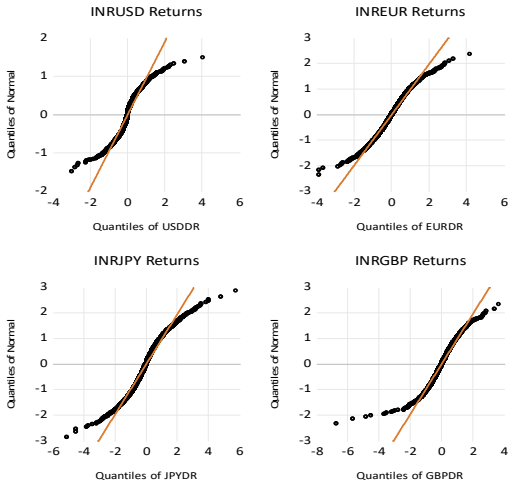

Table. 1. Descriptive Statistics – Returns

	INRUSD	INREUR	INRGBP	INRJPY
Mean	0.011	0.0097	0.006	0.008
Median	0.000	0.004	0.014	0.000
Maximum	4.012	4.155	3.679	5.764
Minimum	-3.006	-3.889	-6.775	-5.123
Std. Dev.	0.397	0.626	0.620	0.762
Skewness	0.202	0.050	-0.564	0.252
Kurtosis	10.828	5.484	9.790	6.848
Jarque-Bera	14949.590	1504.2	11526.64	3663.9
Probability	0.000000	0.000	0.000	0.000
Sum	66.744	56.3851	35.142	50.648
Sum Sq. Dev.	918.400	2291.312	2247.337	3386.023
Observations	5839	5839	5839	5839

Note: Kurtosis >3 implies fat tailed distribution. ***, **,* denotes level of significance at 1%, 5%,and 10 %.Jarque-Bera : H_0 : Skewness and Kurtosis of data follow normal distribution ~ chi-square distribution with 2 d.o.f.

Table 2. Correlation of returns

	Forex Markets			
	INRUSD	INRGBP	INREUR	INRJPY
INRUSD	1			
INRGBP	0.334698	1		
INREUR	0.314129	0.616635	1	
INRJPY	0.530384	0.30191	0.3809	1

Table 3. Unit Root Test Results

Variable	ADF				PP			
	Levels		First Difference		Level		First Difference	
	Test Statistic	Constant trend (*p* value)	Test Statistic	Constant+ trend (*p* value)	Test Statistic	Constant+ trend (*p* value)	Test Statistic	Constant +trend (*p* value)
lnUSD	-1.5665	0.80	-36.070	0.000***	-1.7283	0.7388	-76.3512	0.000***
lnEUR	-3.4189	0.04**	-76.940	0.000***	-3.3992	0.515*	-76.9393	0.000***
lnGBP	-3.0723	0.11	-74.903	0.000***	-3.0723	0.1131	-74.8904	0.000***
lnJPY	-2.4956	0.33	-78.767	0.000***	-2.3940	0.3826	-78.8218	0.000***
INRUSD	-36.07	0.00***						
INREUR	-76.93	0.0001***						
INRGBP	-74.91	0.0001***						
INRJPY	-78.85	0.0001***						

Notes: (*)Significant at the 10%; (**)Significant at the 5%; (***) Significant at the 1%. and (no) Not Significant
*MacKinnon (1996) one-sided p-values. Z denotes the log return of exchange rate pair.

Table 4. Ljung-Box Test for the return's residuals

Exchange Rates	P Values	Stat	C-value
INRUSD Residuals	0.000	86.84	31.41
INREUR Residuals	0.018	35.50	31.41
INRYEN Residuals	0.011	37.27	31.41
INRGBP Residuals	0.003	41.90	31.41

H0: H_0:$\rho_1=\rho_2=\ldots=\rho_m=0$ i.e., first *m* autocorrelations are jointly zero

Figure.3. ACF for returns and squared returns

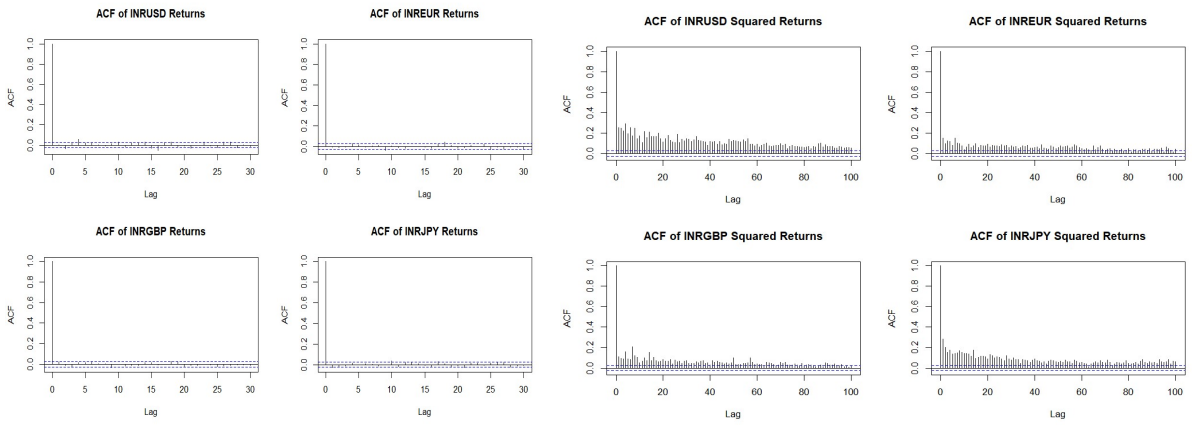

Appendix 4

4.1. Estimation Results

a) Comparing GARCH, EGARCH and GJR to account for the symmetric, asymmetric volatility in exchange rate returns

Table 5. Conditional Covariance Comparisons : GARCH, EGARCH, GJR-GARCH[33]

VARIABLE	GARCH(1,1)			
	Constant	ARCH(1)	GARCH(1,1)	
USDDR	0.001	0.222***	0.778***	
GBPDR	0.007	0.060***	0.916***	
EURDR	0.001	0.0461***	0.946***	
JPYDR	0	0.0851***	0.890***	
	EGARCH			
	Constant	ARCH(1)	GARCH(1,1)	Leverage
USDDR	-0.316	0.4361***	0.971***	0.036***
GBPDR	-0.184	0.134***	0.981***	0.006*
EURDR	-0.118	0.109***	0.988***	0.0106***
JPYDR	-0.326	0.188***	0.966***	0.0257***
	GJR			
	Constant	ARCH(1)	GARCH(1,1)	Leverage
USDDR	0.001	0.252***	0.777***	-0.059
GBPDR	0.007	0.064***	0.920***	-0.01
EURDR	0.003	0.050***	0.946***	-0.01
JPYDR	0.001	0.104***	0.889***	-0.041

Table. 5.b. Identifying optimal model based on minimum AIC and BIC values

		GARCH	**EGARCH**	**GJR**
USDDR	Log likelihood	2.5200	2.5316	2.5208
	AIC	-5.0393	-5.0624*	-5.0409
	BIC	-5.0347	-5.0597*	-5.0382
GBPDR	Log likelihood	2.1245	2.1252	2.1245
	AIC	-4.2484	-4.2495*	-4.2882
	BIC	-4.2464	-4.2469*	-4.2456
EURDR	Log likelihood	2.1100	2.1098	2.1102
	AIC	-4.2194	-4.2188	-4.2196*
	BIC	-4.2174*	-4.2161	-4.2169*
JPYDR	Log likelihood	2.0233	2.0235	2.0240
	AIC	-4.059	-4.0463	-4.0473*
	BIC	-4.0439	-4.0436	-4.0446*

Note: Decision rule → least AIC and BIC values * implies the optimal model based on minimum AIC and BIC values

[33] For cross-market comparisons, results available on request.

Figure.4. Breakpoint Identification using PELT Algorithm

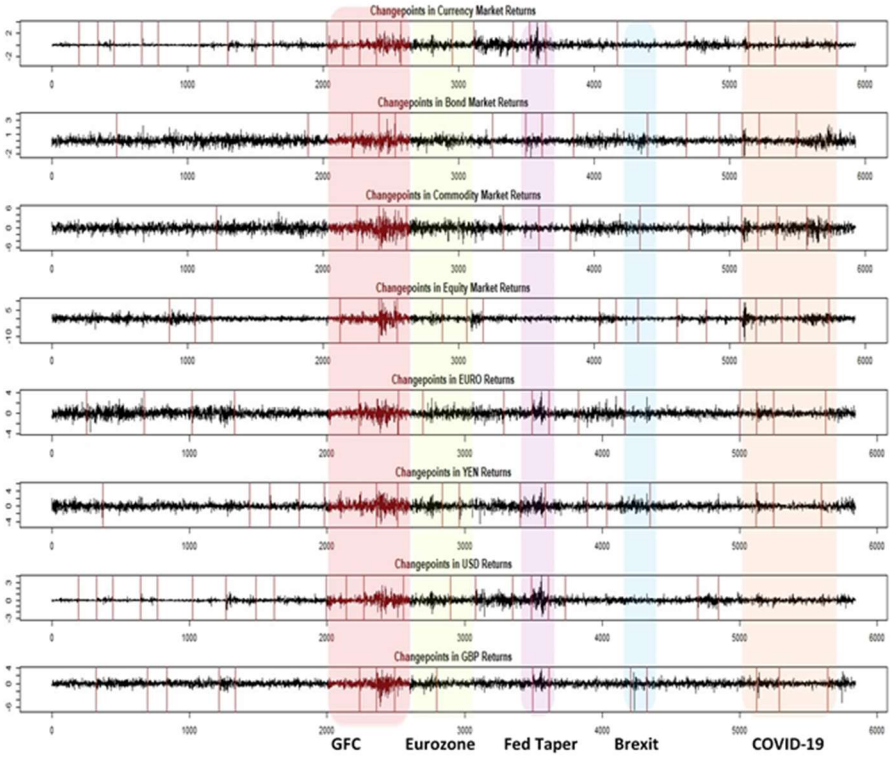

Table. 6. Event intervals considered for testing changes in volatility across scales based on PELT

Financial Distress Events	• Asian Financial Crisis and Dot com Bubble (1999 - 2001) • GFC (Aug 2007-Aug 2009) • Taper Tantrum (22 May – 31 August, 2013) • COVID-19 and Russia Ukraine War (2020-2023)
Normal Period	• Pre GFC (2003-2006) • Post GFC (2009-2015)

4.2. DCC GARCH - Conditional Correlation Results

Figure 5.a. Time varying conditional correlations between exchange rates

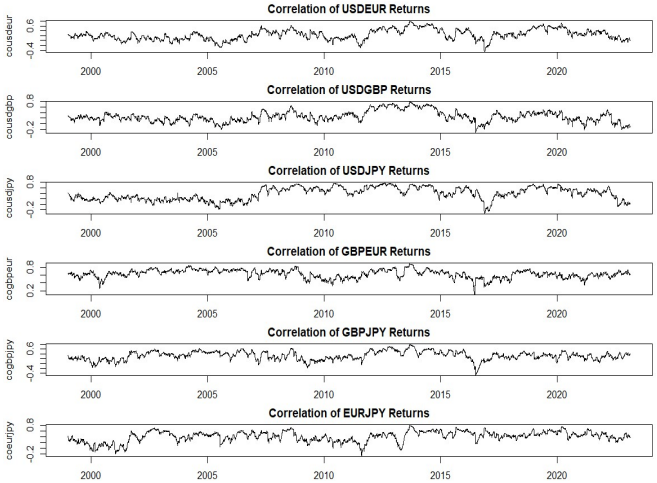

Fig. 5.b. Conditional Covariance in Exchange Rate Returns

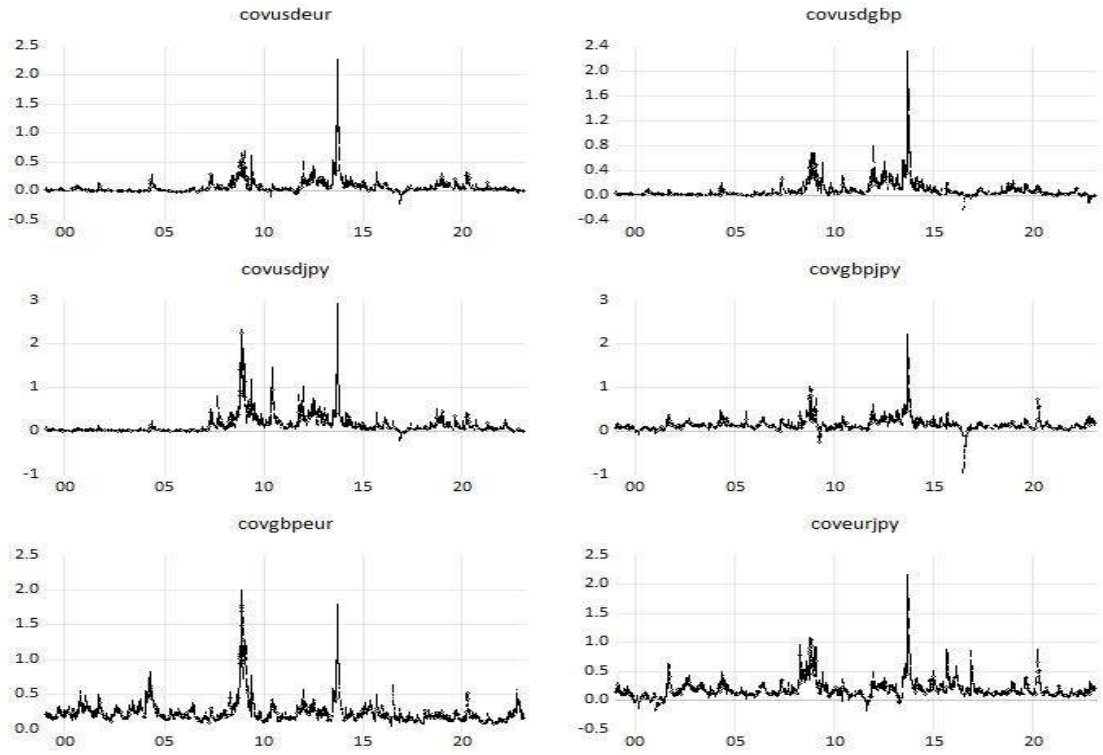

Fig.6. Raw Periodogram and Smoothened Welch periodogram

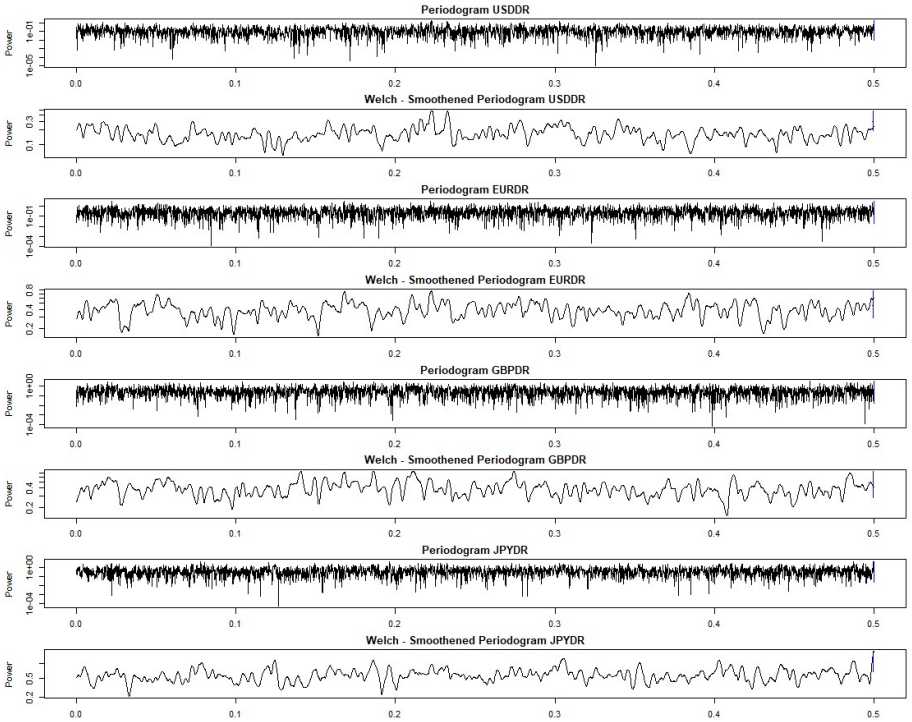

Table 9. Spectral Analysis of Exchange Rate Returns: Power Distribution across events

		INRUSD		INREUR		INRGBP		INRJPY	
	Events	**Max**	**Deviation**	**Max**	**Deviation**	**Max**	**Deviation**	**Max**	**Deviation**
	Aggregate Series	0.0023		0.003		0.00285		0.0064	0
Financial Distress Events	Asian Financial Crisis and Dot com Bubble (1997 - 2001)	0.0020	0.000	0.036	-0.033	0.011	-0.008	0.024	-0.018
	GFC (2007-2009)	0.0250	-0.023	0.066	-0.063	0.048	-0.045	0.123	-0.117
	Eurozone Debt Crisis(2010 - Apr 2011)	0.0130	-0.011	0.022	-0.019	0.036	-0.033	0.056	-0.050
	Taper Tantrum (2013)	0.1600	**-0.158**	0.150	**-0.147**	0.250	**-0.247**	0.27	**-0.264**
	Brexit (June 2016-2017)	0.0058	-0.004	0.028	-0.025	0.044	-0.041	0.075	-0.069
	COVID-19 and Russia Ukraine War (2020-2023)	0.0033	-0.001	0.005	-0.002	0.005	-0.002	0.009	-0.003
Normal Period	Pre GFC (2003-2006)	0.0016	0.001	0.013	-0.010	0.008	-0.005	0.0114	-0.005
	Post GFC (2009-2015)	0.0047	-0.002	0.015	-0.012	0.008	-0.005	0.0215	-0.015
	2015-2020	0.0018	0.001	0.007	-0.005	0.010	-0.007	0.0118	-0.005

Note: Here a more negative deviation implies greater and more aggressive volatility in the returns of the series

Figure.7.b. MODWT Decomposition of Exchange Rates

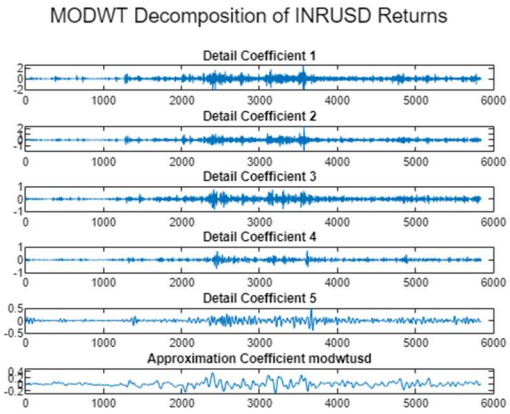

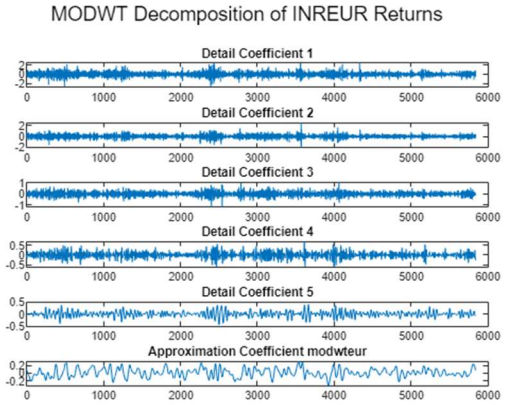

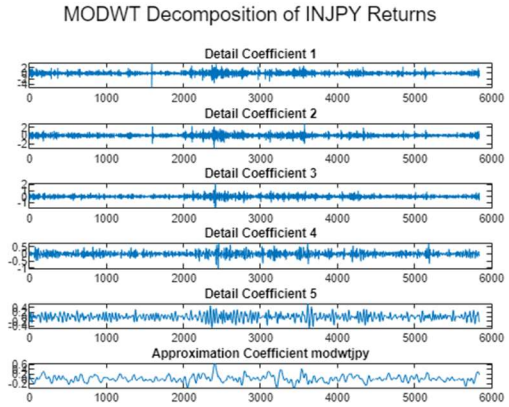

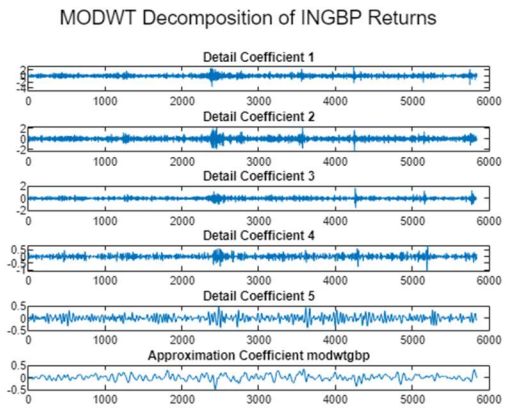

4.3. Crises Specific variance across scale in the currency market

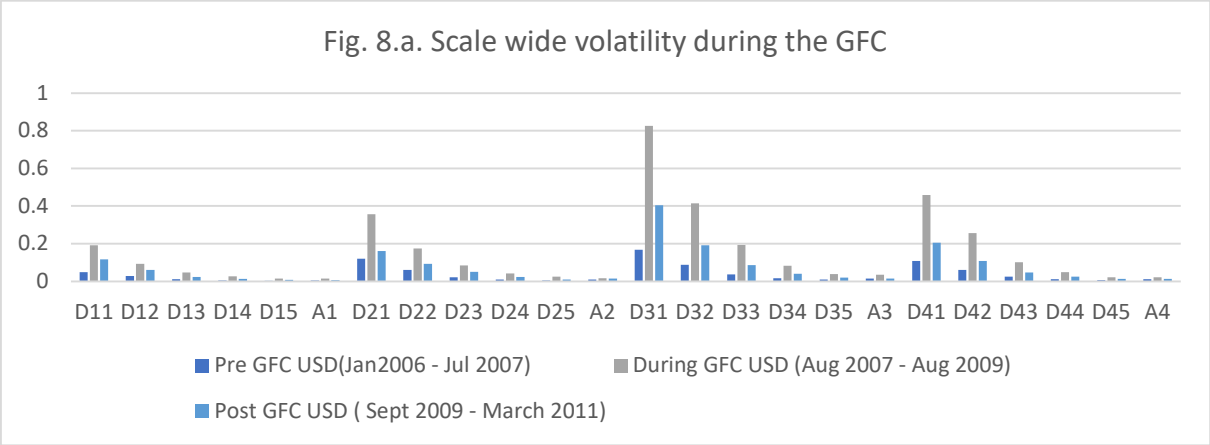

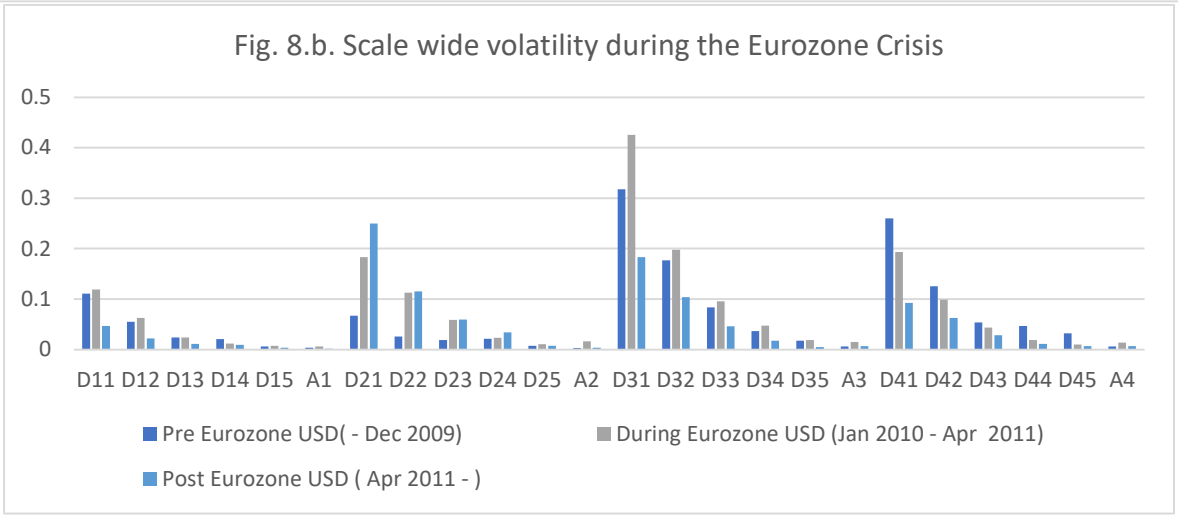

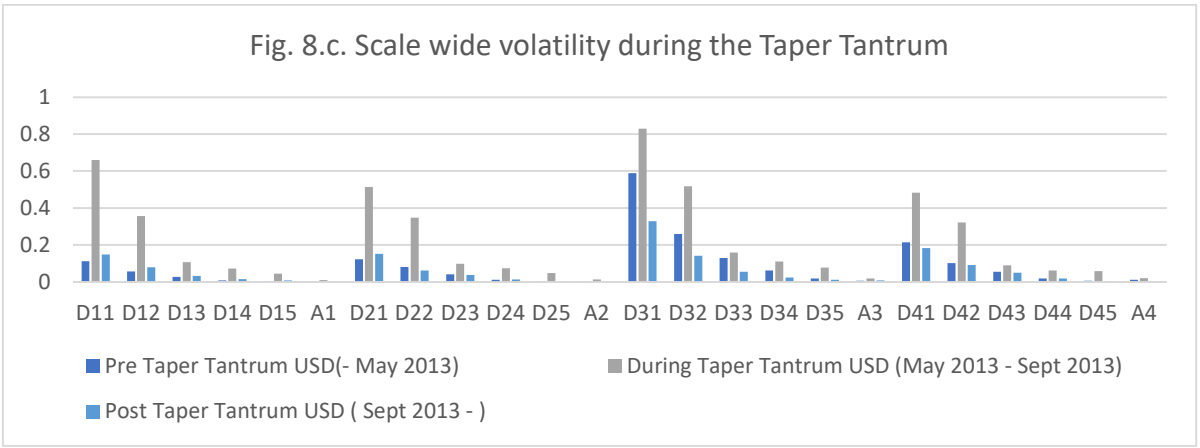

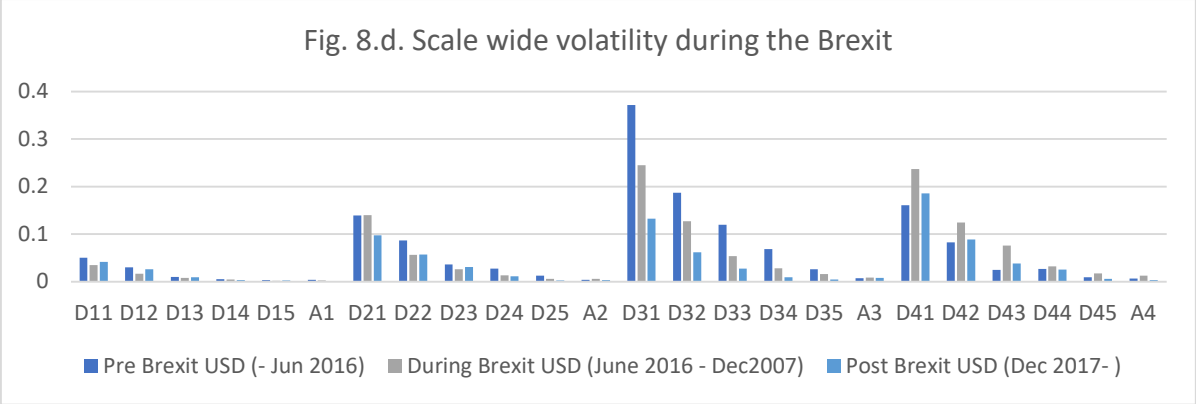

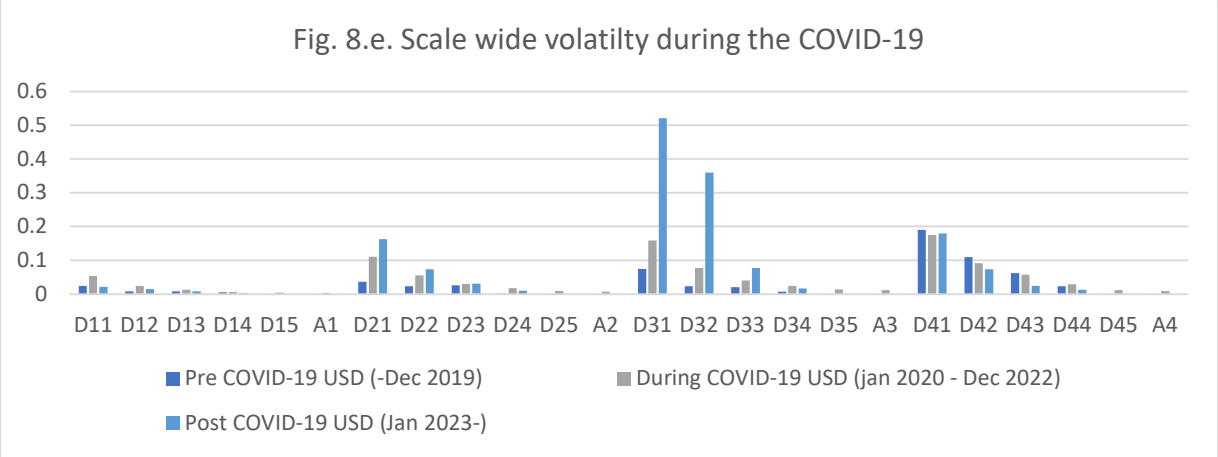

Source: Authors' own compilation

Table 10. Spectral Causality at Different Scales (Breitung and Candelon, 2006)

Null Hypothesis	Test Statistic	Critical Value (p-value)	Decision
INRUSD does not Granger cause INREUR	8.431	6.00 (0.014)	Causality Exists **
INREUR does not Granger cause INRUSD	9.43	6.00 (0.009)	Causality Exists ***
INRUSD does not Granger cause INRJPY	1.76	6.00(0.413)	No Causality
INRJPY does not Granger cause INRUSD	0.941	6.00(0.624)	No Causality
INRUSD does not Granger cause INRGBP	3.96	6.00(0.138)	No Causality
INRGBP does not Granger cause INRUSD	13.42	6.00(0.001)	Causality Exists***
A1 does not Granger causes A2	1.53	6.00(0.463)	No Causality
A2 does not Granger causes A1	3.68	6.00(0.158)	No Causality
A1 does not Granger causes A3	7.94	6.00(0.018)	Causality Exists**
A3 does not Granger causes A1	6.630	6.00(0.036)	Causality Exists**
A1 does not Granger causes A4	3.36	6.00(0.165)	No Causality
A4 does not Granger causes A1	7.96	6.00(0.187)	No Causality
D21 does not Granger causes D11	14.97	6.00(0.006)	Causality Exists ***
D11 does not Granger causes D21	19.41	6.00(0.000)	Causality Exists ***
D31 does not Granger causes D11	1.26	6.00(0.533)	No causality
D11 does not Granger causes D31	5.13	6.00 (0.076)	No Causality
D41 does not Granger causes D11	26.35	6.00 (0.000)	Causality Exists ***
D11 does not Granger causes D41	6.81	6.00(0.033)	Causality Exists**
D22 does not Granger causes D12	0.29	6.00(0.864)	No Causality
D12 does not Granger causes D22	6.87	6.00(0.032)	Causality Exists**
D32 does not Granger causes D12	1.64	6.00 (0.439)	No Causality
D12 does not Granger causes D32	7.23	6.00 (0.026)	Causality Exists**
D42 does not Granger causes D12	0.91	6.00(0.633)	No Causality
D12 does not Granger causes D42	46.55	6.00(0.000)	Causality Exists***
D23 does not Granger causes D13	1.11	6.00(0.572)	No Causality
D13 does not Granger causes D23	0.24	6.00(0.886)	No Causality

D33 does not Granger causes D13	13.45	6.00(0.001)	Causality Exists***
D13 does not Granger causes D33	15.27	6.00(0.005)	Causality Exists***
D43 does not Granger causes D13	3.44	6.00(0.179)	No Causality
D13 does not Granger causes D43	12.12	6.00(0.002)	No Causality
D24 does not Granger causes D14	4.85	6.00(0.088)	No Causality
D14 does not Granger causes D24	2.03	6.00(0.361)	No Causality
D34 does not Granger causes D14	15.86	6.00(0.00)	Causality Exists***
D14 does not Granger causes D34	0.02	6.00(0.989)	No Causality
D44 does not Granger causes D14	10.00	6.00(0.006)	Causality Exists***
D14 does not Granger causes D44	7.15	6.0(0.027)	Casuality Exists**
D25 does not Granger causes D15	1.92	6.00 (0.382)	No Causality
D15 does not Granger causes D25	7.85	6.00(0.0197)	Causality Exists**
D35 does not Granger causes D15	0.92	6.00(0.630)	No Causality
D15 does not Granger causes D35	4.32	6.00(0.114)	No Causality
D45 does not Granger causes D15	10.00	6.00()	Causality Exists**
D15 does not Granger causes D45	8.04	6.00(0.017)	Causality Exists**

Note:: ***, **, and * denote statistical significance at 1%, 5%, and 10% level, respectively

4.4. Forecasting Results

Table 13.a. Multiscale Forecasting using MODWT: Random walk vs ARIMA/ARMA vs GARCH vs Hybrid LSTM- wavenet with MRA

GARCH 1,1 05-01-1999 to 15-01-2023								
	USDDR		**EURDR**		**JPYDR**		**GBPDR**	
	RMSE	**MAE**	**RMSE**	**MAE**	**RMSE**	**MAE**	**RMSE**	**MAE**
USDDR	0.216	0.172	0.481	0.35	0.916	0.683	0.446	0.34
Approximation	0.003	0.002	0.007	0.006	0.006	0.005	0.012	0.012
D1	0.128	0.098	0.31	0.223	0.766	0.631	0.372	0.282
D2	0.132	0.107	0.254	0.223	0.254	0.223	0.235	0.177
D3	0.039	0.029	0.078	0.064	0.247	0.195	0.104	0.076
D4	0.033	0.028	0.059	0.053	0.039	0.028	0.073	0.064
D5	0.006	0.005	0.012	0.009	0.211	0.157	0.019	0.015
ARMA Identification								
	USDDR		**EURDR**		**JPYDR**		**GBPDR**	
	ARMA(P,Q)	**AIC**	**ARMA(P,Q)**	**AIC**	**ARMA(P,Q)**	**AIC**	**ARMA(P,Q)**	**AIC**
Aggregate	5,5	0.98407	3,3	1.9023	3,3	2.2912	3,4	1.882
Approximation	3,3	-12.1955	4,5	-11.5835	5,5	-11.1494	4,4	-11.3236
Di1	2,4	-2.443	0,5	-1.3767	2,3	-1.07561	0,5	-1.4677
Di2	4,5	4.17895	5,5	-3.40229	4,5	-2.96856	5,5	-3.17545
Di3	5,5	-5.4001	2,5	-3.98043	5,4	-3.45316	4,4	-4.2479
Di4	4,5	-7.0554	5,5	-6.03529	2,5	-5.6592	5,5	-5.87591
Di5	4,5	-9.5803	5,5	-8.75005	2,5	-8.38829	2,5	-8.83282
Subsample Static Forecasts using ARMA								
	USDDR		**EURDR**		**JPYDR**		**GBPDR**	
	RMSE	**MAE**	**RMSE**	**MAE**	**RMSE**	**MAE**	**RMSE**	**MAE**
Aggregate	0.21	0.162	0.481	0.351	0.919	0.688	0.447	0.343
Approximation	0.001	0	0.001	0.001	0.001	0.001	0.001	0.001
D1	0.043	0.032	0.122	0.095	0.178	0.137	0.103	0.079
D2	0.018	0.016	0.051	0.044	0.121	0.103	0.038	0.028
D3	0.01	0.008	0.017	0.012	0.048	0.04	0.023	0.017
D4	0.01	0.008	0.011	0.01	0.013	0.011	0.019	0.015
D5	0.002	0.002	0.002	0.002	0.003	0.003	0.003	0.003
Random Walk								
	USDDR		**EURDR**		**JPYDR**		**GBPDR**	
	RMSE	**MAE**	**RMSE**	**MAE**	**RMSE**	**MAE**	**RMSE**	**MAE**
Aggregate	0.209	0.166	0.48	0.351	0.916	0.684	0.446	0.34

Approximation	0.003	0.002	0.007	0.006	0.007	0.006	0.012	0.011
D1	0.129	0.098	0.311	0.224	0.766	0.63	0.372	0.282
D2	0.132	0.107	0.254	0.223	0.591	0.527	0.235	0.177
D3	0.039	0.029	0.078	0.064	0.247	0.194	0.104	0.076
D4	0.033	0.028	0.059	0.053	0.039	0.028	0.073	0.064
D5	0.006	0.005	0.012	0.009	0.025	0.021	0.018	0.014

Table. 13.b. Wavelet based machine learning forecast results for aggregate series of returns

Model	**INRUSD**		**INREUR**		**INRJPY**		**INRGBP**	
	RMSE	**MAE**	**RMSE**	**MAE**	**RMSE**	**MAE**	**RMSE**	**MAE**
GARCH	**0.216**[c]	0.172	**0.481**[d]	0.35	0.916	0.683	0.446[a]	0.34
ARMA	**0.21**[b]	0.162	0.481	0.351	0.919	0.688	0.447[c]	0.343
Random Walk	**0.209**[a]	0.161	**0.48**[c]	0.351	0.916	0.684	0.446[b]	0.34
LSTM - Test	0.299	0.22	**0.45**[b]	0.343	**0.568**[c]	0.624	0.585	0.422
LSTM- Validation	0.39	0.291	0.484	0.3704	0.624	0.44	0.641	0.4846
LSTM + MRA – Test (db2)	**0.224**[d]	0.186	0.724	0.666	**0.864**[d]	0.839	0.692	0.639
LSTM + MRA – Validation (db2)	0.252	0.0.199	0.708	0.64	0.864	0.839	0.735	0.653
LSTM Hybrid Wavenet - Test	0.299	0.22	**0.449**[a]	0.342	**0.563**[b]	0.398	**0.568**[d]	0.404
LSTM Hybrid Wavenet - Validation	0.39	0.29	0.483	0.369	0.611	0.436	0.633	0.474
Hybrid LSTM Wavenet with MRA-Test (db2)	2.34	2.32	2.784	2.76	2.507	2.476	6.457	6.441
Hybrid LSTM Wavenet with MRA-Validation (db2)	1.865	1.808	3.355	3.299	4.019	3.979	6.678	6.632
LSTM + MRA – Test(sym8)	0.545	0.524	1.098	1.071	**0.354**[a]	0.3643	0.733	0.689
LSTM + MRA – Validation(sym8)	0.552	0.5259	1.098	1.068	0.364	0.312	0.773	0.705
Hybrid LSTM Wavenet with MRA- Test (sym10)	4.608	4.607	4.09	4.081	6.639	6.624	5.807	5.788
Hybrid LSTM Wavenet with MRA-Validation (sym10)	4.102	4.078	4.85	4.819	6.742	6.694	7.321	7.28

Figure 12. Currency pair in ascending order for the model errors based on validation scores